cmgh
CELLULAR AND MOLECULAR GASTROENTEROLOGY AND HEPATOLOGY

ORIGINAL RESEARCH

The Development of Spasmolytic Polypeptide/TFF2-Expressing Metaplasia (SPEM) During Gastric Repair Is Absent in the Aged Stomach

Amy C. Engevik,[1] Rui Feng,[1] Eunyoung Choi,[2] Shana White,[3] Nina Bertaux-Skeirik,[1] Jing Li,[1] Maxime M. Mahe,[4] Eitaro Aihara,[1] Li Yang,[1] Betsy DiPasquale,[5] Sunghee Oh,[6] Kristen A. Engevik,[1] Andrew S. Giraud,[7] Marshall H. Montrose,[1] Mario Medvedovic,[3] Michael A. Helmrath,[4] James R. Goldenring,[2,§] and Yana Zavros[1,§]

[1]Department of Molecular and Cellular Physiology, [3]Department of Environmental Health, Division of Biostatistics and Bioinformatics, University of Cincinnati College of Medicine, Cincinnati, Ohio; [2]Nashville VA Medical Center, Department of Surgery, Department of Cell and Developmental Biology, Epithelial Biology Center, Vanderbilt University Medical Center, Nashville, Tennessee; [4]Division of Pediatric Surgery, [5]Pathology Research Core, Cincinnati Children's Hospital Medical Research Center, Cincinnati, Ohio; [6]Department of Computer Science and Statistics, Jeju National University, Jeju, South Korea; [7]Murdoch Childrens Research Institute, The Royal Children's Hospital, Melbourne, Victoria, Australia

SUMMARY

This study demonstrates the emergence of spasmolytic polypeptide/TFF2-expressing metaplasia during regeneration of the gastric epithelium. The development of spasmolytic polypeptide/TFF2-expressing metaplasia in response to injury is absent in the aged stomach. In addition, transplantation of gastric organoids promoted gastric regeneration.

BACKGROUND & AIMS: During aging, physiological changes in the stomach result in more tenuous gastric tissue that is less capable of repairing injury, leading to increased susceptibility to chronic ulceration. Spasmolytic polypeptide/trefoil factor 2–expressing metaplasia (SPEM) is known to emerge after parietal cell loss and during *Helicobacter pylori* infection, however, its role in gastric ulcer repair is unknown. Therefore, we sought to investigate if SPEM plays a role in epithelial regeneration.

METHODS: Acetic acid ulcers were induced in young (2–3 mo) and aged (18–24 mo) C57BL/6 mice to determine the quality of ulcer repair with advancing age. Yellow chameleon 3.0 mice were used to generate yellow fluorescent protein–expressing organoids for transplantation. Yellow fluorescent protein–positive gastric organoids were transplanted into the submucosa and lumen of the stomach immediately after ulcer induction. Gastric tissue was collected and analyzed to determine the engraftment of organoid-derived cells within the regenerating epithelium.

RESULTS: Wound healing in young mice coincided with the emergence of SPEM within the ulcerated region, a response that was absent in the aged stomach. Although aged mice showed less metaplasia surrounding the ulcerated tissue, organoid-transplanted aged mice showed regenerated gastric glands containing organoid-derived cells. Organoid transplantation in the aged mice led to the emergence of SPEM and gastric regeneration.

CONCLUSIONS: These data show the development of SPEM during gastric repair in response to injury that is absent in the aged stomach. In addition, gastric organoids in an injury/transplantation mouse model promoted gastric regeneration. *(Cell Mol Gastroenterol Hepatol 2016;2:605–624; http://dx.doi.org/10.1016/j.jcmgh.2016.05.004)*

Keywords: Epithelial Regeneration; Gastric Cancer; Human Gastric Organoids; CD44v.

During aging, changes in the stomach result in gastric tissue that is less capable of repairing injury correctly. These changes include decreased gastric acid secretion, motility, and proliferation.[1] In addition, angiogenesis, a fundamental process essential for wound healing, is impaired with advanced age.[2–4] Such pathophysiological changes are believed to result in disrupted repair in response to chronic ulceration in the elderly that can be exacerbated during chronic insults such as *Helicobacter pylori* infection or nonsteroidal anti-inflammatory drug administration.[5] In elderly patients there is a strong

§Authors share co-senior authorship.

Abbreviations used in this paper: **CD44v, variant isoform of CD44; Cftr, cystic fibrosis transmembrane conductance regulator; CgA, chromagranin A; Clu, Clusterin; Ctss, cathepsin S; Dmbt1, deleted in malignant brain tumors 1; DMEM, Dulbecco's modified Eagle medium; DPBS, Dulbecco's phosphate buffered saline; ES, enrichment score; Gpx2, glutathione peroxidase 2 (gastrointestinal); GSEA, gene set enrichment analysis; GSII, *Griffonia simplicifolia II*; hFGO, human-derived fundic gastric organoid; HK, hydrogen potassium adenosine triphosphatase; IF, intrinsic factor; Mad2l1, MAD2 mitotic arrest deficient-like 1; Mmp12, matrix metallopeptidase 12 (macrophage elastase); PBS, phosphate-buffered saline; qRT-PCR, quantitative reverse-transcription polymerase chain reaction; SPEM, spasmolytic polypeptide expressing metaplasia; TFF, trefoil factor; TX, Triton X-100 in PBS; UEA1, ulex europaeus; Wfdc2, WAP 4-disulfide core domain 2; YFP, yellow fluorescent protein.**

Most current article

2352-345X
http://dx.doi.org/10.1016/j.jcmgh.2016.05.004

association between ulceration with cancer or evolution of dysplasia into neoplasia.[6] Renewal of gastric stem cells to produce committed progenitor cells that differentiate further into adult epithelial cell types is important for the structural integrity of the mucosa. However, relatively little is known regarding the age-related changes affecting gastric epithelial stem cells. Early studies have shown that in aged rats, stem cell proliferation and epithelial cell numbers are decreased compared with young animals,[7] thus suggesting impaired tissue integrity in the aged stomach.

The origin of cells for repair of severe gastric epithelial injury has not received extensive attention. Recent investigations have indicated that loss of parietal cells, either from acute toxic injury or chronic *Helicobacter* infection, leads to the development of spasmolytic polypeptide/trefoil factor (TFF) 2–expressing metaplasia (SPEM) through transdifferentiation of chief cells into mucous cell metaplasia.[8,9] In the face of continued inflammation and M2-macrophage influence, SPEM may progress to a more proliferative preneoplastic metaplasia.[10] However, studies with acute injury have indicated that SPEM disappears after resolution of injury.[11] Whether SPEM may contribute to the healing of gastric ulcers is unknown. We now report that SPEM represents a major reparative lineage responsible for wound healing after gastric ulcer injury. In addition, the healing of gastric ulcers in the aged stomach is promoted by the transplantation of gastric organoids.

Materials and Methods

Mouse-Derived Gastric Organoid Culture

Gastric organoids were generated as previously described.[12–14] Yellow chameleon 3.0 mice were used to generate yellow fluorescent protein (YFP)-expressing organoids for transplantation. Briefly, the stomach was opened along the greater curvature and washed in phosphate-buffered saline (PBS). A dissecting microscope was used to remove the muscle layer. The remaining tissue was cut into pieces smaller than 5 mm^2 and incubated in 5 mmol/L EDTA in Dulbecco's phosphate buffered saline (DPBS) (without Ca^{2+} and Mg^{2+}) for 2 hours on a shaker at 4°C. For gastric gland dissociation 5 mL of dissociation buffer (55 mmol/L D-sorbitol and 43 mmol/L sucrose in DPBS without Ca^{2+} and Mg^{2+}) was added to tissue and vigorously shaken for 2 minutes. Media containing glands was centrifuged at 65 × g for 5 minutes. Glands were resuspended in Matrigel Corning Incorporated (Tewksbury, MA) and 50 μL of glands suspended in Matrigel was added to each well. Gastric organoid media containing 50% Wnt conditioned media, 10% R-spondin conditioned media, [Leu15]-gastrin 1 (10 nmol/L; Tocris, Pittsburgh, PA), N-acetylcysteine (1 mmol/L; Sigma, St. Louis, MO), fibroblast growth factor 10 (100 ng/mL; PeproTech, Rocky Hill, NJ), epidermal growth factor (50 ng/mL; PeproTech), Noggin (100 ng/mL; PeproTech), Y-27632 (10 μmol/L; Sigma), and advanced Dulbecco's modified Eagle medium (DMEM)/F12 was added after Matrigel polymerization at 37°C. Organoids were cultured 7 days before transplantation. The L cells were a kind gift from Drs Meritxell Huch, Sina Bartfeld, and Hans Clevers (Hubrecht Institute for Developmental Biology and Stem Cell Research, The Netherlands). The modified human embryonic kidney–293T cells were donated by Dr Jeffrey Whitsett (Section of Neonatology, Perinatal and Pulmonary Biology, Cincinnati Children's Hospital Medical Center and The University of Cincinnati College of Medicine, Cincinnati, OH).

Human-Derived Gastric Organoid Culture

Gastric organoids were generated as previously described.[15] Human fundic gastric tissue was obtained from Cincinnati Children's Hospital with patient consent. Patients were aged between 15 and 19 years. Human fundus was collected during sleeve gastrectomies (Institutional Review Board protocol number: 2013-2251). The human gastric tissue was cut into pieces smaller than 5 mm^2 before being suspended in advanced DMEM/F12 supplemented with 20 mmol/L HEPES and 2 mmol/L Glutamax (Thermo Fisher Scientific). A total of 1 mg/mL collagenase (C9891; Sigma) and 2 mg/mL bovine serum albumin were added to the supplemented advanced DMEM/F12 media. The solution was placed on a stir plate in a water bath at 37°C with oxygen for 30 minutes. The tissue was strained through mesh to collect the gastric glands and remove any undigested tissue. Gastric glands were washed with DPBS (without Ca^{2+} and Mg^{2+}) containing antibiotics. Isolated gastric glands were embedded in Matrigel and overlayed with organoid growth media containing 30% advanced DMEM/F12, 10 mmol/L HEPES, 2 mmol/L Glutamax, 1× N2, 1× B27, 1 mmol/L N-acetylcysteine, 10 mmol/L nicotinamide, 50 ng/mL epidermal growth factor, 100 μg/mL Noggin, 10% R-spondin conditioned media, 50% Wnt conditioned media, 100 μg/mL fibroblast growth factor 10, 1 nmol/L gastrin, 1% penicillin/streptomycin, 50 mg/mL kanamycin, 0.25 mg/mL amphotericin B, 10 mg/mL gentamicin, and 10 μmol/L Y-27632.

Acetic Acid–Induced Gastric Injury and Organoid Transplantation

All mouse studies were approved by the University of Cincinnati Institutional Animal Care and Use Committee, which maintains an American Association of Assessment and Accreditation of Laboratory Animal Care facility. Young mice (age, 2–3 mo) and aged mice (age, >18 mo) (C57BL/6) were subjected to acetic acid gastric injury as previously described.[16] Briefly, mice were anesthetized with isoflurane. The stomach was exteriorized through a midline abdominal laparotomy opening. One hundred percent acetic acid was applied to the serosal surface of the exteriorized stomach for 25 seconds using a capillary tube. Organoids were transplanted at the same injury site. Before transplantation, organoids were washed twice with ice-cold DPBS (without Ca^{2+} and Mg^{2+}) to remove Matrigel. Organoids then were resuspended in DPBS to a concentration of approximately 500 organoids per 50 μL. Immediately after ulcer induction either 50 μL DPBS or 50 μL organoids were injected into the muscle and submucosa of the stomach surrounding the ulcer site using a 26G × 3/8 syringe (309625; Thermo Fisher, Waltham, MA). The stomach then was replaced into the

abdominal cavity and the muscle and skin incisions were sutured.

Immunofluorescence

Tissue was collected from the ulcerated area and fixed in Carnoy's fixative or 4% paraformaldehyde for 16 hours. Human gastric ulcer tissue array was purchased from US Biomax, Inc (Rockville, MD) (BB01011a). Longitudinal sections of the mouse stomach were paraffin-embedded and 4-μm sections were stained for histologic evaluation. Slides were deparaffinized and placed in boiling antigen retrieval solution (0.01 mol/L sodium citrate buffer) for 10 minutes. Twenty percent normal goat, donkey, or rabbit serum was used to block the sections. Sections then were immunostained with a primary antibody overnight at 4°C, followed by incubation with a secondary antibody for 1 hour. The primary antibodies and dilutions used were as follows: 1:200 dilution of anti–green fluorescent protein Alexa Fluor 488 antibody (A21311; Thermo Fisher), 1:10,000 mouse-specific rat anti-CD44v, 1:25,000 human-specific rat anti-CD44v (a gift from Professor Hideyuki Saya, Keio University), 1:1000 mouse anti–hydrogen potassium adenosine triphosphatase β (MA3-923; Affinity Bioreagents, Golden, CO), 1:100 rabbit anti-intrinsic factor (Ab91322; Abcam, Cambridge, MA), 1:100 rabbit anti–chromagranin A (CgA) (Ab15160; Abcam), and rabbit antihistone (Ab125027; Abcam). Rabbit anti-TFF2 (mouse- and human-specific) was adsorbed overnight at 4°C with 5 μg recombinant human TFF2 in a final volume of 5 μL and used at a 1:1000 dilution for immunostaining. Secondary antibodies used were diluted 1:100 anti-goat Alexa Fluor 488, anti-rabbit Alexa Fluor 488, 555, or 633, and anti-mouse Alexa Fluor 633. Hoechst (10 mg/mL) was added after the secondary antibody in a 1:1000 dilution and incubated for 30 minutes at room temperature. To identify the expression of surface mucous pit cells, slides were stained with 20 μg/mL ulex europaeus (UEAI) fluorescein isothiocyanate conjugate. *Griffoni simplicifolia II* (GSII) Alexa Fluor 647 (20 μg/mL) was used to assess the presence of mucous neck cells and the emergence of SPEM. Coverslips were mounted onto slides with Vectashield mounting medium (H-1400; Vector Laboratories, Inc, Burlingame, CA) and analyzed with a Zeiss (San Diego, CA) LSM710 LIVE Duo Confocal Microscope.

Laser Capture Microdissection

Tissue was collected from the ulcerated and uninjured/intact area and fixed in 4% paraformaldehyde overnight at 4°C. Longitudinal sections of the mouse stomach were paraffin-embedded and 4-μm sections were stained according to the manufacturer's protocol using the HistoGene Laser Capture Microdissection Frozen Section Staining Kit (cat. KIT0401; Applied Biosystems, Thermo Fisher Scientific). Laser capture microdissection was used to confirm the expression of YFP at the ulcer margin and intact epithelium regions of the tissue. Tissues were collected using the Molecular Devices/Arcturus Veritas Laser-Capture Microdissection System (Sunnyvale, CA) (model 704). Briefly, the UV cutting laser was used to trace around the region of interest, and an infrared laser (setting, 90 mW; pulse, 300 μsec) was used to capture cells. RNA was extracted from captured tissue using Arcturus Paradise Extraction and Isolation (cat. RA7001; Applied Biosystems) according to the manufacturer's protocol, and analyzed as detailed for quantitative reverse-transcription polymerase chain reaction (qRT-PCR).

qRT-PCR

Total RNA was isolated from mouse or human stomach–derived gastric glands or organoids using TRIzol (Life Technologies, Thermo Fisher Scientific) according to the manufacturer's protocol. A High Capacity Complementary DNA Reverse Transcription Kit synthesized complementary DNA from 100 ng RNA (Applied Biosystems). qPCR was performed according to the manufacturer's protocol. Primers used for PCR using human stomach–derived gastric organoids or glands were as follows: hypoxanthine guanine phosphoribosyl transferase (Hs02800695_m1; Life Technologies), ATP4B (Hs01026288_m1), pepsinogen (Hs00160052_m1), Gast (Hs01099852_g1), Muc 5AC (Hs00873651_mH), Muc6 (Hs01674026_g1), clusterin (Hs00156548_m1), HE4 (Hs00899484_m1), and TFF2 (Hs00193719_m1). Primers used for PCR using mouse stomach–derived gastric organoids or glands were as follows: deleted in malignant brain tumors 1 (Dmbt1) (Mm00455996_m1), matrix metallopeptidase 12 (macrophage elastase) (Mmp12) (Mm00500554_m1), clusterin (Mm01197002_m1), MAD2 mitotic arrest deficient-like 1 (Mad2l1) (Mm00786984_s1), cystic fibrosis transmembrane conductance regulator (Cftr) (Mm00445197_m1), cathepsin S (Ctss) (Mm01255859_m1), Pgc (Mm01278038_m1), WAP 4-disulfide core domain 2 (Wfdc2) (Mm00509434_m1), glutathione peroxidase 2 (gastrointestinal) (Gpx2) (Mm00850074_g1), YFP (Mr04329676_Mr), and TFF2 (Mm00447491_m1). Amplification was performed in duplicate wells using a StepOne Real-Time PCR System (Applied Biosytems). Fold change was calculated as follows: (Ct-Ct high) = n target, 2ntarget/2nHPRT = fold change, where Ct is the threshold cycle.

Whole Mount Tissue Immunostaining

Mouse stomachs were harvested 30 days after injury and fixed in 4% paraformaldehyde at 4°C for 16 hours. Stomachs then were washed with PBS 3 times, and the desired tissue was cut to stain. Tissue was placed in Dent's solution (1:4, dimethyl sulfoxide to methanol) for 1 hour with gentle rotation at room temperature. At 4°C the tissue then was incubated in 75%, 50%, and then 25% methanol in PBS for 15 minutes each. Tissue then was washed 3 times in 1% Triton X-100 (Thermo Fisher Scientific) in PBS (TX), and blocked in 5% goat serum made in TX for 2 hours at 4°C with rotation. Tissue then was incubated with a 1:50 dilution of H+,K+–adenosine triphosphatase antibody (Santa Cruz Biotechnology, Dallas, TX) at 4°C for 16 hours. Tissue was washed in TX for an hour 3 times, and incubated with secondary antibody goat anti-rabbit Alexa Fluor 633 at a dilution of 1:200 at 4°C for 16 hours. Tissue was washed for 1 hour in TX twice, and incubated with Hoechst (10 μg/mL) made in TX for 1 hour at 4°C. Tissue then was washed in TX

for 30 minutes, and transferred to 50% methanol/PBS for 15 minutes, 100% methanol for 15 minutes, and stored in fresh methanol at 4°C. Ten minutes before imaging, tissue was placed in a glass chamber slide in Murrays Clearing solution (2:1, benzyl benzoate:benzyl alcohol) and imaged using a Zeiss LSM710 LIVE Duo Confocal Microscope.

RNA Sequencing

Gastric tissue was collected from the ulcerated region and from the adjacent uninjured side of the stomach. The collected tissue was homogenized in 1 mL of TRIzol. The RNeasy micro kit (74004; Qiagen, Valencia, CA) was used to extract RNA. A total of 1 μg of total RNA, measured by the Invitrogen (Thermo Fisher Scientific) Qbit high-sensitivity spectrofluorometric measurement, was poly A–selected and reverse-transcribed using Illumina's (San Diego) TruSeq stranded messenger RNA library preparation kit. After 15 cycles of PCR amplification, completed libraries were sequenced on an Illumina HiSeq2500 in Rapid Mode. The result was 10 million or more high-quality, 50-base long, single-end reads per sample.

Bioinformatics RNA-Sequencing Data Analysis

Sequence reads were aligned to the reference mouse genome (mm10) using the TopHat aligner.[17] Reads aligning to each known transcript were counted and all follow-up analysis was performed using Bioconductor packages for next-generation sequencing data analysis.[18] The data have been submitted to a public repository (GEO accession number: GSE73336). The differential gene expression analysis was performed based on the negative-binomial statistical model of read counts as implemented in the Bioconductor packages *edgeR* (ulcerated vs uninjured samples)[19] and *DESeq* (organoid vs fundic tissue samples).[20] Significance tests are not considered for the organoid vs fundic tissue samples because the groups consist of single replicates (fold change is reported). The significance of differential expression between ulcerated and uninjured samples was assessed using the simple generalized linear model with a single factor (ulcerated: yes or no). *P* values are reported without adjustment for multiple comparison because the gene list is prehypothesized.

The gene set enrichment analysis (GSEA) enrichment plots and enrichment score statistics were generated via the GSEA Java desktop application available from the Broad Institute (significance was assessed using 1000 random permutations of gene labels).[21] The *P* values for the traditional over-representation analysis of gene lists are derived by the Fisher exact test as implemented in R (where the number of significant genes in the entire data set and in each list is the number of genes [in either category] with unadjusted *P* values less than .05 for differential expression).

Fluorescence-Activated Cell Sorting

Whole stomach was collected from mice transplanted with YFP gastric organoids for 5 months. Gastric glands were isolated as described for mouse-derived organoid culture. Isolated gastric glands were resuspended in DPBS (without Ca^{2+} and Mg^{2+}), and gland suspension was passed through a 26G needle for a single-cell suspension. Cells then were filtered using a 40-μm filter. To identify YFP-positive, organoid-derived cells, the single-cell suspension was stained with a 1:50 dilution of green fluorescent protein Alexa Fluor 488 for 20 minutes at room temperature. Cells then were washed with DPBS (without Ca^{2+} and Mg^{2+}) and resuspended in mouse organoid growth media with 10 μmol/L Y-27632 and without Wnt and R-Spondin for sorting. Cell sorting was performed on a Fluorescence-Activated Cell Sorting (FACS)Aria II (BD Bioscience, San Jose, CA). An unstained control was used for gating. YFP+ and YFP- cells were collected and cultured as described in mouse-derived organoid culture.

Statistical Analysis

The results were tested for significance by either a 1-way analysis of variance or an unpaired *t* test using commercially available software (GraphPad Software; GraphPad Prism, San Diego, CA). A *P* value less than .05 was considered significant.

Results

Aged Mice Show Impaired Wound Healing in Response to Gastric Injury

To identify differences in healing that arise from advancing age, gastric ulcers were induced, through application of acetic acid, in the stomachs of young (age, 2–3 mo) and aged (age, >18 mo) mice. Histology of uninjured gastric tissue collected from young (Figure 1*A*, left panel) and aged mice (Figure 1*A*, right panel) showed similar morphology. Stomachs then were examined 1–30 days after ulcer induction to assess gastric repair. The gross morphology and histology of stomachs corresponding to both young (Figures 1*B*, left panel, and 2*A*) and aged (Figures 1*B*, right panel, and 2*B*) mice showed a distinct ulcer margin adjacent to the denuded tissue 1 day after injury. Young (Figures 1*C*, left panel, and 2*C*) and aged (Figures 1*C*, right panel, and 2*D*) mice maintained prominent ulcer margins surrounding the damaged tissue 3 days after injury. Although in young mice we observed re-epithelialization of the damaged tissue (Figures 1*D*, left panel, and 2*E*), aged mice showed a prominent ulcer margin 7 days after injury (Figures 1*D*, right panel, and 2*F*). Histologic evaluation showed that 30 days after injury, stomachs of young mice showed typical characteristics of epithelial repair that included re-epithelialization of the gastric mucosa and epithelial regeneration (Figure 1*E*, left panel). In contrast to the regeneration of the gastric epithelium observed in the young mice, stomachs collected from the aged mice showed severe foveolar hyperplasia (Figure 1*E*, right panel). Measurement of the ulcerated area showed a significant reduction of ulcer size in young mice 7 days after injury (Figure 1*F*). Ulcer size in aged mice showed no significant difference 7 days after injury compared with initial ulcer size 1 day after ulcer induction (Figure 1*F*). Compared with young mice, aged

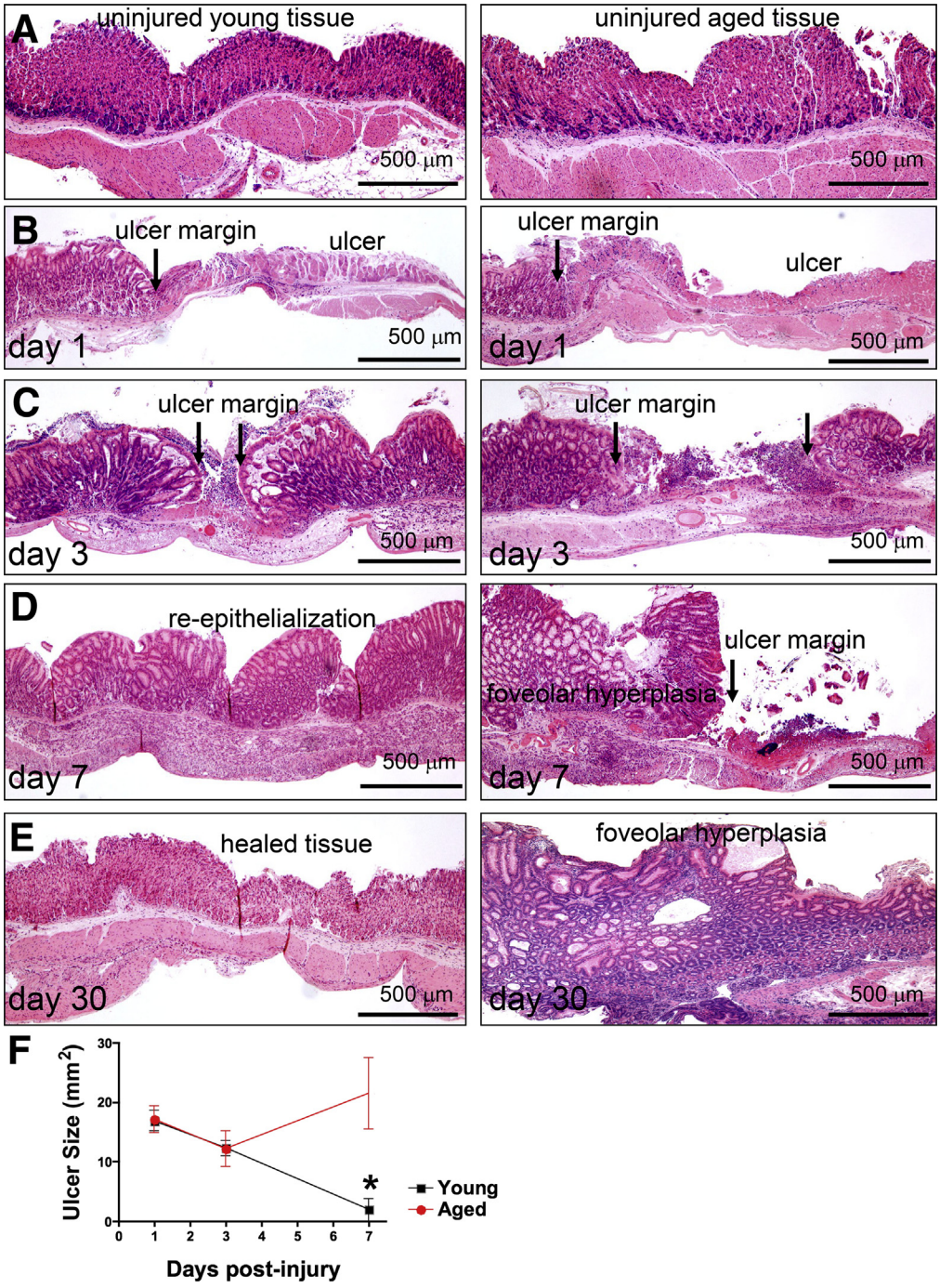

Figure 1. Histologic changes in gastric tissue of young and aged mice in response to acetic acid–induced injury. (*A*) H&E staining of gastric tissue from young and aged mice. Uninjured and ulcerated tissue of young and aged mice at (*B*) 1, (*C*) 3, (*D*) 7, and (*E*) 30 days after injury are shown. *Arrows* indicate ulcer margin. (*F*) Ulcer sizes from young (black) and aged (red) mice at 1, 3, and 7 days after injury. **P* < .05 compared with the young group, N = 3–6 mice per time point using a 2-way analysis of variance. *Scale bars*: 500 μm.

mice had significantly greater ulcer size 7 days after injury (Figure 1*F*).

To identify further differences in gastric epithelial repair between young and aged mice, immunofluorescence staining was used to quantify the expression of gastric cell lineages including surface mucous pit (UEAI), parietal (HK), and endocrine (CgA) cells. Immunofluorescence staining in young mice 30 days after injury showed the re-expression of surface mucous, parietal, and endocrine cells within the regenerating epithelium (Figure 3*A* and *D*). However, we noted that the distribution of surface mucous and parietal cells did not return to numbers before injury (Figure 3*A* and *D*). In contrast, aged mice showed expansion of surface mucous cells within the injured epithelium accompanied by diminished parietal cells and loss of normal gastric gland architecture 30 days after injury (Figure 3*B* and *E*). Uninjured gastric tissue from young and aged (Figure 3*F*) mice showed comparable numbers of parietal cells and endocrine cells, and increased numbers of surface mucous cells in the aged stomach (Figure 3*C*). Collectively, these data

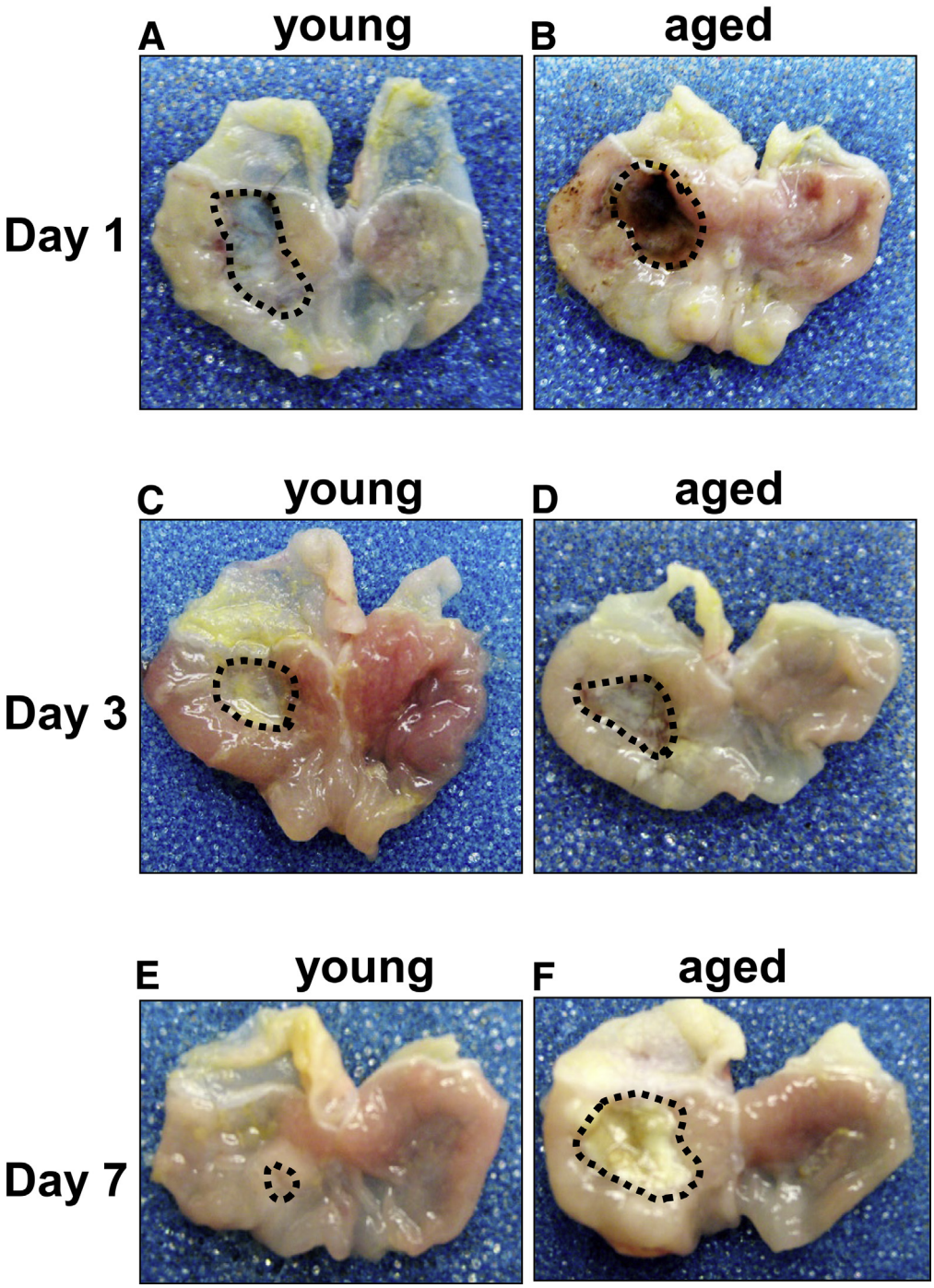

Figure 2. Gross morphologic changes in gastric tissue of young and aged mice in response to acetic acid–induced injury. Gross morphology of gastric tissue from young and aged mice at (*A* and *B*) 1, (*C* and *D*) 3, and (*E* and *F*) 7 days after injury. Highlighted areas indicate ulcerated tissue. Representative of N = 4 mice per time point.

suggest that aging results in a decreased capacity to promote normal epithelial regeneration in the stomach in response to injury.

Ulcer Healing Is Associated With the Development of SPEM

To identify alterations in gene expression attendant with gastric injury, RNA sequencing was performed using RNA isolated from uninjured tissue and tissue collected from the ulcerated region of stomachs collected from young mice. Genes were chosen based on previously published data sets of markers of SPEM lineages.[9,22] The significance of expression for genes associated with SPEM in comparison with genes not included in these categories was performed via GSEA.[21] The enrichment scores (ES) and *P* values for the ES were 0.55 and .02, respectively, for the SPEM genes. The positive ES values and low *P* values suggest that these genes, as a set, are up-regulated significantly in the ulcerated samples (Figure 4*A*). A heat map

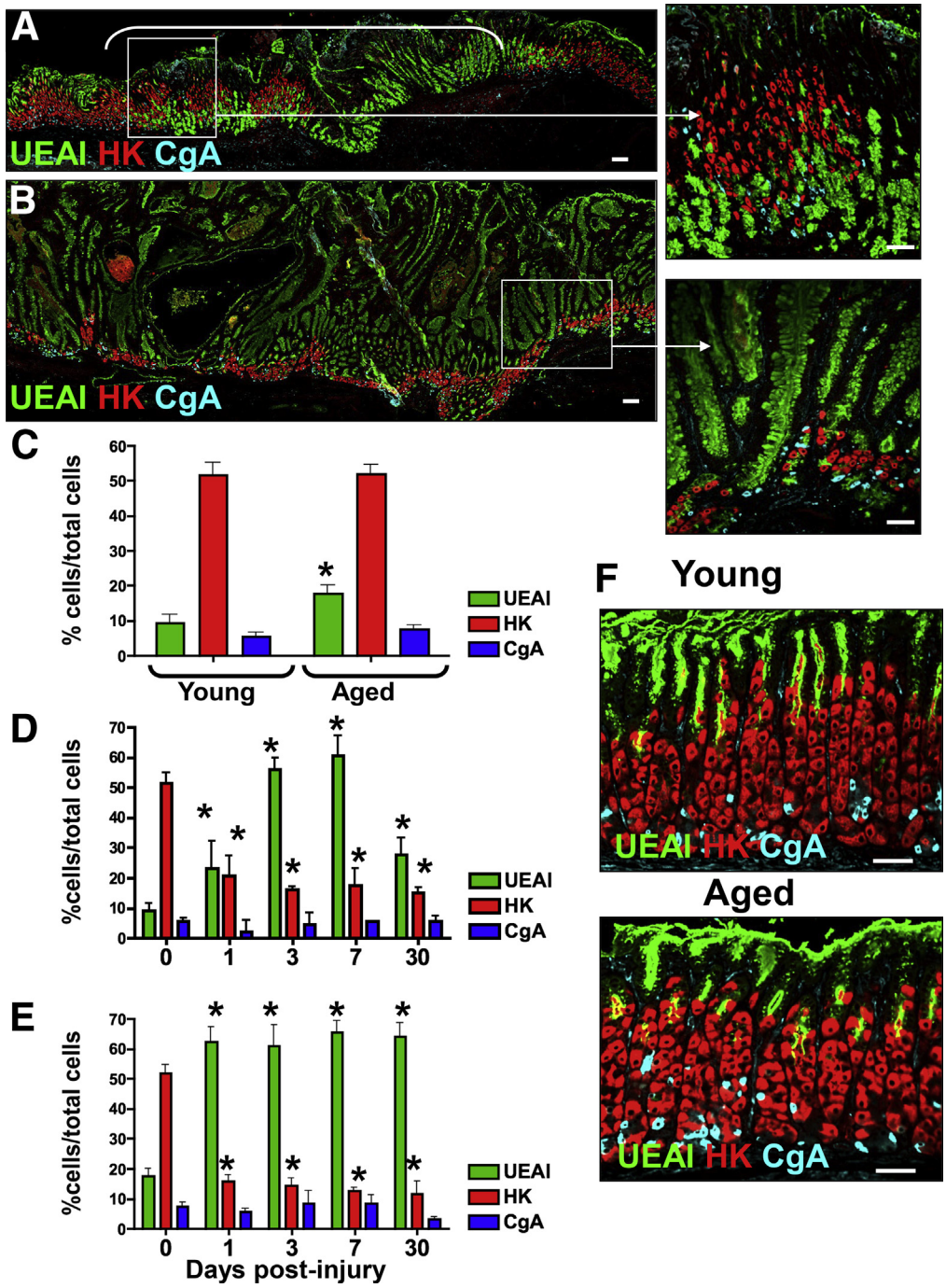

Figure 3. Expression of gastric cell lineages within the ulcerated gastric tissue of young and aged mice. Sections of injured gastric tissue collected from (*A*) young and (*B*) aged mice were immunostained for UEAI (surface mucous pit cells, green), HK (parietal cells, red), and CgA (endocrine cells, blue) 30 days after injury. Morphometric analysis of UEAI, HK, and CgA-positive cells per field in (*C*) uninjured stomach tissue, and ulcerated tissue at 1, 3, 7, and 30 days after injury in (*D*) young and (*E*) aged mice. (*F*) Uninjured tissue collected from young and aged mouse stomachs. *$P < .05$ compared with uninjured tissue (0 days after injury), N = 3–4 mice per time point. *Scale bars*: 50 μm.

comparing the expression profiles of uninjured and ulcerated tissues 7 days after injury showed a significant increase in a number of transcripts, 7 days after injury, that have been implicated in the emergence of SPEM in the ulcerated region (Figure 4*B*). Figure 4*A* and *B* show that 7 days after injury there was a prominent up-regulation of a number of transcripts including Dmbt1, Mmp12, clusterin (Clu), Mad2I1, Cftr, Ctss, Wfdc2 (HE4), and Gpx2, thus indicative of SPEM development.[9,23] qRT-PCR data validated the increase in Dmbt1, Mmp12, Clu, Mad2I1, Cftr, Ctss, Wfdc2 (HE4), and Gpx2 observed in the injured tissue compared with the uninjured control (Figure 5*A*).[9] GSEA also was performed to determine the significance of expression for genes associated with SPEM induced by inflammation; this gene set included a subset of the genes in the previous SPEM set specific to inflammation.[21] The ES and *P* values were 0.80 and less than .001, respectively, for the SPEM with inflammation gene set (Figure 5*B*). A heat map comparing the expression profiles of both uninjured and injured tissues also showed a significant increase in a number of genes associated with SPEM induced by inflammation (Figure 5*C*). Genes were chosen based on

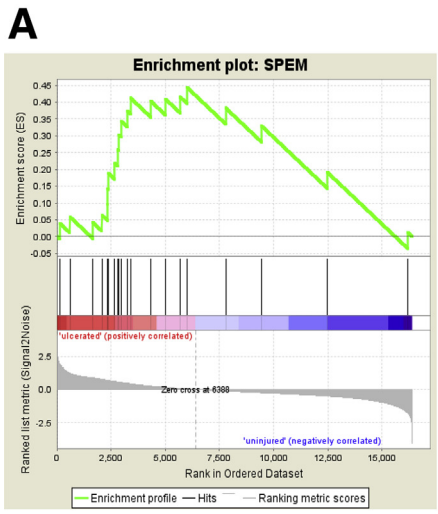

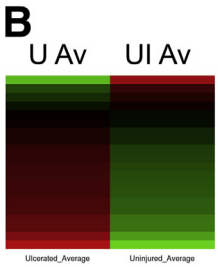

Gene Symbol	Fold Change	*P*-value
Pgc	0.091	*P* < .001
Cxcl17	0.665	.126
Traf4	0.960	.825
Etv5	1.008	.976
Chek2	1.092	.744
Cenpk	1.111	.754
Slfn9	1.236	.402
Ndc1	1.160	.518
Clu	1.768	.111
Vil1	1.558	.111
Ube2c	1.500	.082
Ccnb2	1.427	.121
Top2a	1.434	.059
Gpx2	1.777	.036
Mmp12	2.353	.031
Wfdc2	2.492	.001
Dmbt1	4.567	*P* < .001
Mad2l1	1.535	.061
Cftr	6.519	*P* < .001
Ctss	3.592	*P* < .001

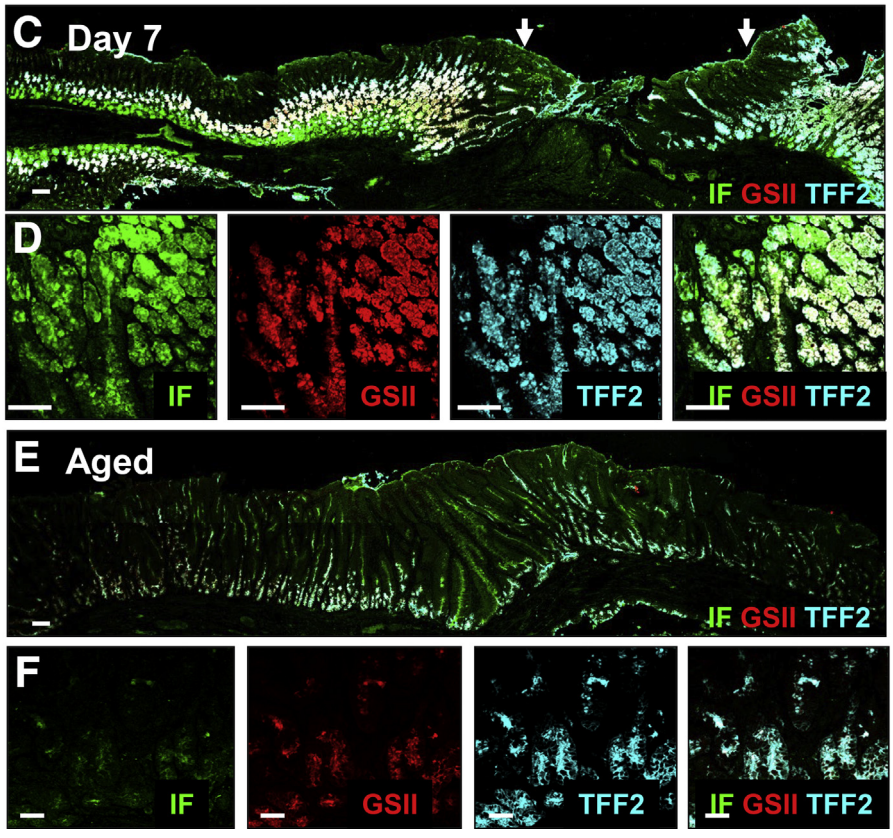

Figure 4. Emergence of SPEM in regenerating gastric tissue after acetic acid–induced injury. RNA sequencing of uninjured and injured gastric tissue from young mice. (*A*) Gene set enrichment analysis. (*B*) Heat map depicting average standardized reads per kilobase per million for gene expression changes in SPEM-associated genes. Table shows fold change of up-regulated transcripts associated with the emergence or progression of SPEM. *P* values were generated by the Fisher exact test as implemented in R. (*C*) Immunofluorescence staining for SPEM using intrinsic factor (green) co-labeled with GSII-lectin (red) and TFF2 (blue) 7 days after injury. *Arrows* indicate the ulcer margin. (*D*) Higher magnification is shown. Immunofluorescence staining for SPEM using IF (green) co-labeled with GSII-lectin (red) and TFF2 (blue) in ulcerated gastric tissue 7 days after injury in aged mice. (*E*) Immunofluorescence staining for SPEM using tissue collected from an aged stomach 7 days after injury. (*F*) Higher magnification images of IF, GSII, and TFF2 in epithelium. *Scale bars*: 50 μm.

previously published data sets of markers of SPEM lineages.[9,22]

To validate the results of the RNA sequencing further, we evaluated the presence of SPEM within the ulcerated gastric tissue using immunofluorescence. SPEM cells have been identified as co-expressing intrinsic factor (IF), TFF2, and mucous neck cell marker GSII-lectin (Figure 4*C* and *D*).[11,24,25] Emerging SPEM cells co-expressing IF and TFF2 with GSII were observed at the base of the glands at the ulcer margin within 24 hours of injury in young mice (data not shown). These IF/TFF2/GSII–expressing cells became obvious at the ulcer margins 3, 5 (data not shown), and 7 days after injury (Figure 4*C* and *D*). A higher magnification of the glands appearing at the base of the ulcer margin clearly shows the emergence of SPEM cells (Figure 4*D*). In contrast to the young mice, aged stomachs showed no emergence of SPEM cells (Figure 3*E* and *F*). SPEM also was confirmed by the characterization of GSII and IF expression in distinct granules. Although the prezymogenic cells showed hybrid granules containing zymogenic and mucous components,[26] we observed that in the injured tissue SPEM cells showed separate granules (Figure 6*A*).[11] To examine the emergence of SPEM during gastric ulceration, the

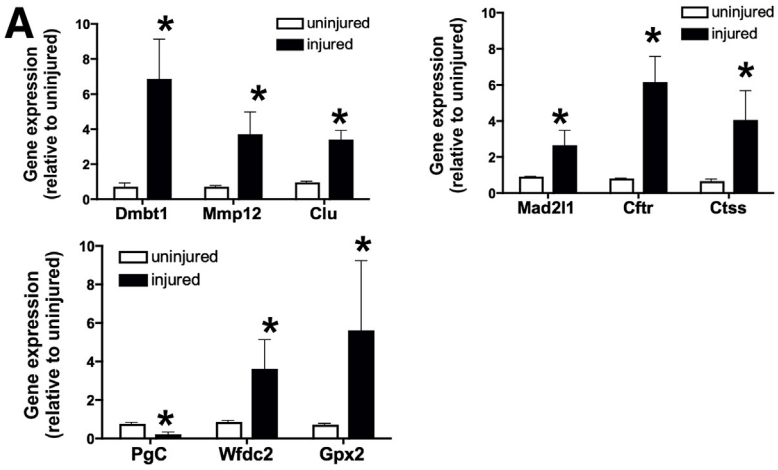

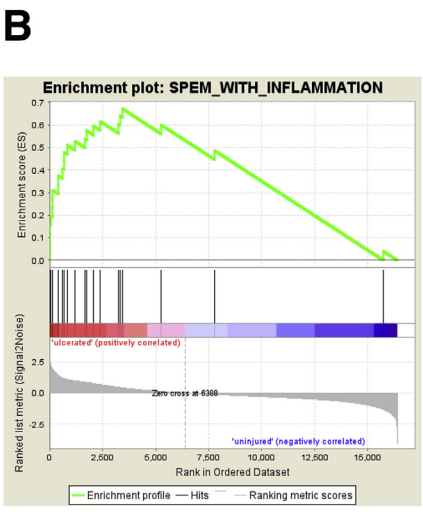

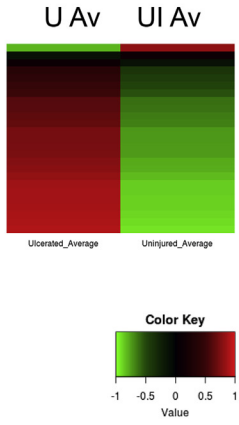

Gene Symbol	Fold Change	*P*-value
Ceacam10	0.494	.014
Etv5	1.008	.976
Prom1	1.148	.627
Il18r1	1.430	.136
Vil1	1.558	.111
Ly6a	1.317	.153
Gpx2	1.777	.036
Dmbt1	4.567	*P* < .001
Mad2l1	1.535	.061
Gpa33	2.269	.002
Glipr1	1.846	.011
Muc4	4.257	.001
Cd14	5.308	*P* < .001
Cftr	6.519	*P* < .001
Itga2	3.224	*P* < .001
Casp1	2.700	.002
Arhgap9	2.777	.001
Ms4a6b	3.683	*P* < .001
Tyrobp	3.718	*P* < .001
Ms4a6c	3.349	*P* < .001
Ceacam1	6.071	*P* < .001
Ctss	3.592	*P* < .001
Gpr171	4.841	*P* < .001
Lyz2	4.358	*P* < .001
Pigr	7.716	*P* < .001

Figure 5. Validation of RNA sequencing data. (*A*) qRT-PCR was performed using RNA isolated from uninjured and ulcerated gastric tissue from young mice 7 days after injury. Shown is the average fold change of SPEM-associated genes Dmbt1, Mmp12, Wfdc2 (HE4), Mad2l1, Cftr, Ctss, Gpx2, and clusterin (Clu). *$P < .05$ compared with uninjured tissue, N = 3–4 mice per group using 1 way analysis of variance. (*B*) Heat map depicting average standardized reads per kilobase per million for gene expression changes in SPEM-associated genes. (*C*) Table showing fold change of transcripts corresponding to the emergence or progression of SPEM associated with inflammation. Data are expressed as the means ± SEM. $P < .05$ compared with uninjured tissue (0 days after injury) as measured by 1-way analysis of variance.

expression of the SPEM marker CD44 variant 9 (CD44v9)[27] was investigated. Compared with the uninjured tissue in which CD44v was not expressed (Figure 6*B*), CD44v expression emerged at the ulcer margin 5 days after injury and co-localized with TFF2 (Figure 6*C*).

Transplanted Mouse-Derived Gastric Organoids Contribute to Healing of Gastric Ulcers in the Stomach

Gastric organoids derived from whole stomach glands were transplanted into acetic acid–induced ulcerated gastric tissue of young (age, 2–3 mo) and aged (age, 18–24 mo) mice (Figure 7*A*). To visualize engraftment directly within the gastric epithelium, gastric organoids were derived from the whole stomachs of yellow chameleon 3.0 mice[28]; therefore, the organoids expressed YFP (Figure 7*B*). When compared with injection into the lumen, organoids transplanted into the submucosa of the stomach efficiently promoted repair (Figure 7*C*). In addition, microspheres were cultured in Matrigel and organoid growth media for 4 days, harvested, washed, and transplanted into the stomachs of aged mice after acetic acid–induced injury (Figure 7*D*). Microspheres did not promote repair of the aged gastric epithelium 7 days after injury when compared with organoids (Figure 7*D*).

To identify the pattern of organoid engraftment, immunofluorescence was used to determine the presence of gastric organoid-derived cells in the ulcerated tissue co-expressing SPEM marker CD44v. At 3 and 7 days after injury and transplantation, YFP+ organoid-derived cells were observed within the ulcer margin of aged mice (Figure 8*A* and *B*). Specifically, YFP+ cells were located within the regenerating gastric glands at the base of the ulcer margin, forming glandular structures that covered the submucosa and expressed CD44v (Figure 8*A* and *B*). As the epithelium regenerated, YFP/CD44v-expressing cells decreased and were difficult to identify 30 days after injury (Figure 8*C* and *D*). Engraftment of organoid-derived

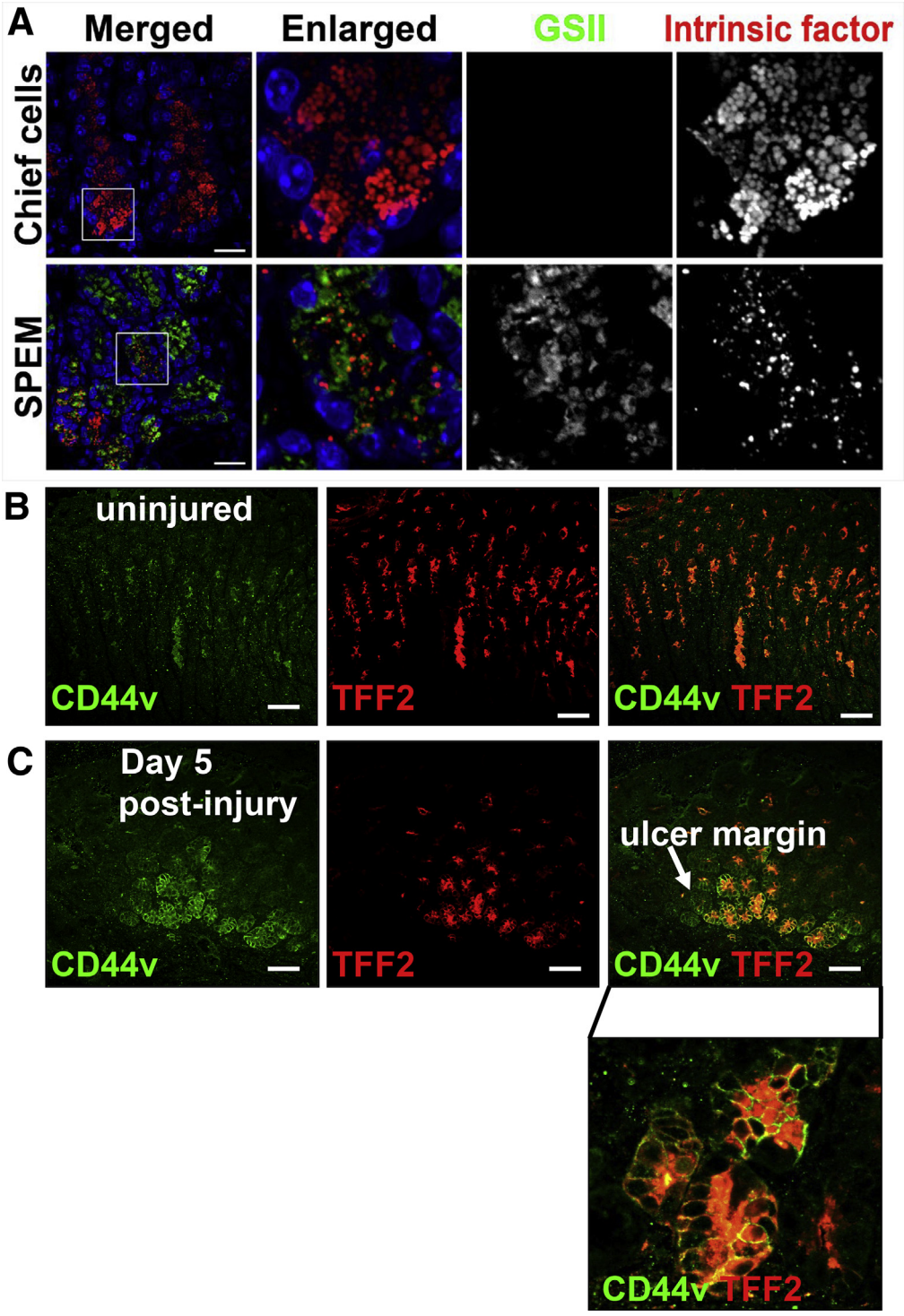

Figure 6. Emergence of SPEM in regenerating gastric tissue after acetic acid–induced injury. (*A*) SPEM within injured tissue as indicated by separate GSII (green) and IF (red) granules. Expression of CD44v (green) and TFF2 (red) in (*B*) uninjured and (*C*) injured gastric epithelium. *Scale bars*: 50 μm.

cells within the submucosa was accounted for by the expression of mesenchymal marker α-smooth muscle actin within the cultured organoids used for transplantation. As previously documented,[14] organoids are composed of both an epithelial and mesenchymal compartment before passaging. YFP+ cells were not observed in untransplanted mice in response to injury (Figure 9*A*).

YFP expression was confirmed by RT-PCR in laser captured microdissected tissue collected at the ulcer margins and was absent in intact/uninjured epithelium of aged mice transplanted with YFP+ gastric organoids (Figure 9*B*). Notably, although in general we observed a loss of engrafted cells in the healed ulcer, in some cases at 30 days after transplantation, YFP+ glands remained

A

Mouse Age	Human Age	Category
2-3 months	20-30 years	Young
10-14 months	38-47 years	Middle aged
18-24 months	56+ years	Aged

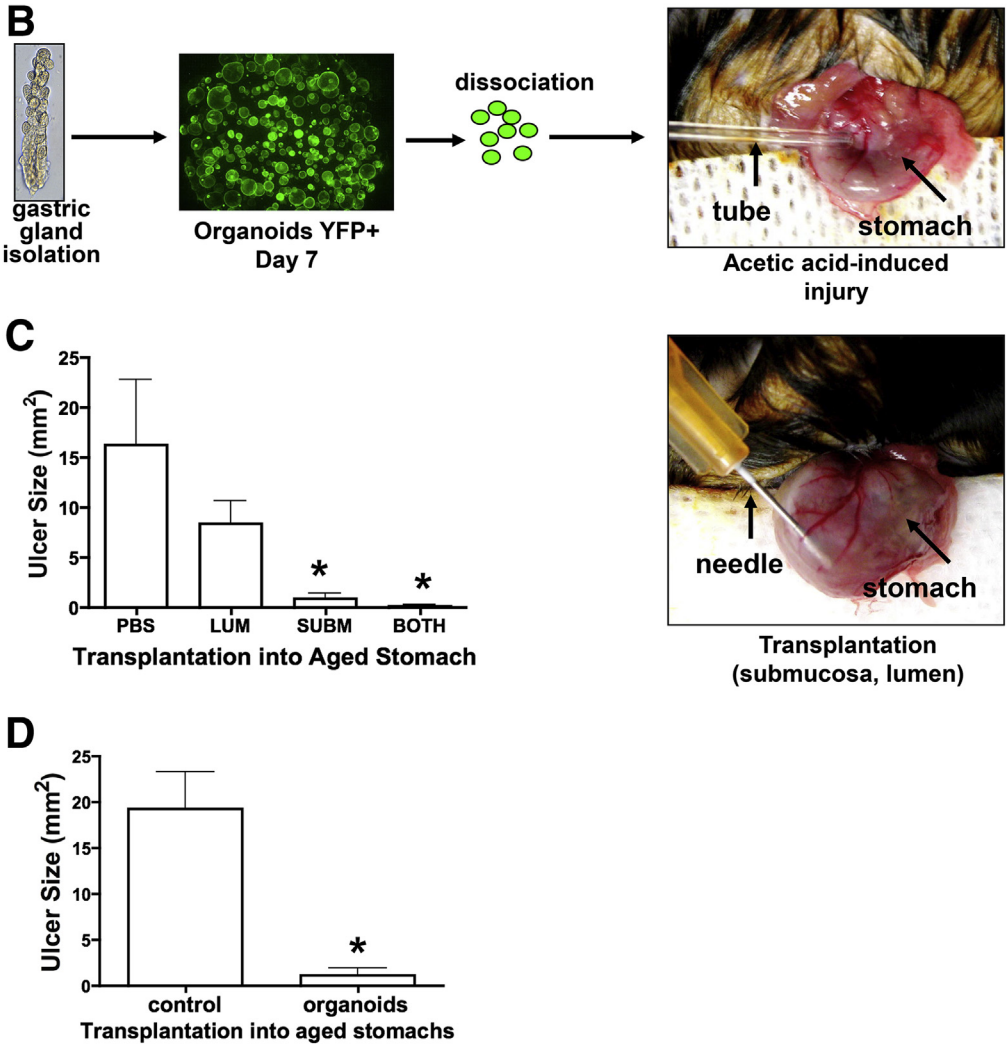

Figure 7. Experimental design and YFP+ gastric organoids. (*A*) Table comparing mouse and human age. (*B*) Experimental protocol. Gastric glands were isolated from mice expressing the YFP transgene. YFP gastric organoids were generated from glands. After 7 days in culture, organoids were dissociated and transplanted into the stomach of aged mice immediately after ulcer induction. (*C*) Gastric organoids were injected within the lumen (LUM), submucosa (SUBM), or both lumen and submucosa of the aged mouse stomach, and ulcer size was measured. *$P < .05$ compared with PBS control, N = 4 mice per group. (*D*) Gastric organoids or microspheres (control) were injected within the submucosa of the aged mouse stomach and ulcer size was measured. Data are expressed as means ± SEM. *$P < .05$ compared to control as assessed by 1-way analysis of variance.

within the regenerating epithelium (Figure 9*D*). Single YFP+ cells sorted by fluorescence-activated cell sorting generated organoids in vitro (Figure 9*D*). Collectively, these data show the successful engraftment of gastric organoids within the gastric epithelium in response to injury.

Immunofluorescence staining was used to quantify the expression of gastric cell lineages including surface mucous (UEAI), parietal (HK), and endocrine (CgA) cells. Immunofluorescence staining in aged mice transplanted with organoids showed the re-expression of surface mucous pit, parietal, and endocrine cells within the repaired epithelium 30 days after injury (Figure 10*A* and *B*). Uninjured gastric tissue from young (Figure 3*C*) and aged mice transplanted with organoids (Figure 10*B*) showed comparable numbers of parietal, surface mucous pit, and endocrine cells. Measurement of the ulcerated area showed a significant reduction of ulcer size in organoid-transplanted aged mice 7 days after injury, comparable with the stomachs collected from young mice (Figure 10*C*). Ulcers measured in the aged mouse stomachs did not heal within 7 days after injury (Figure 10*C*).

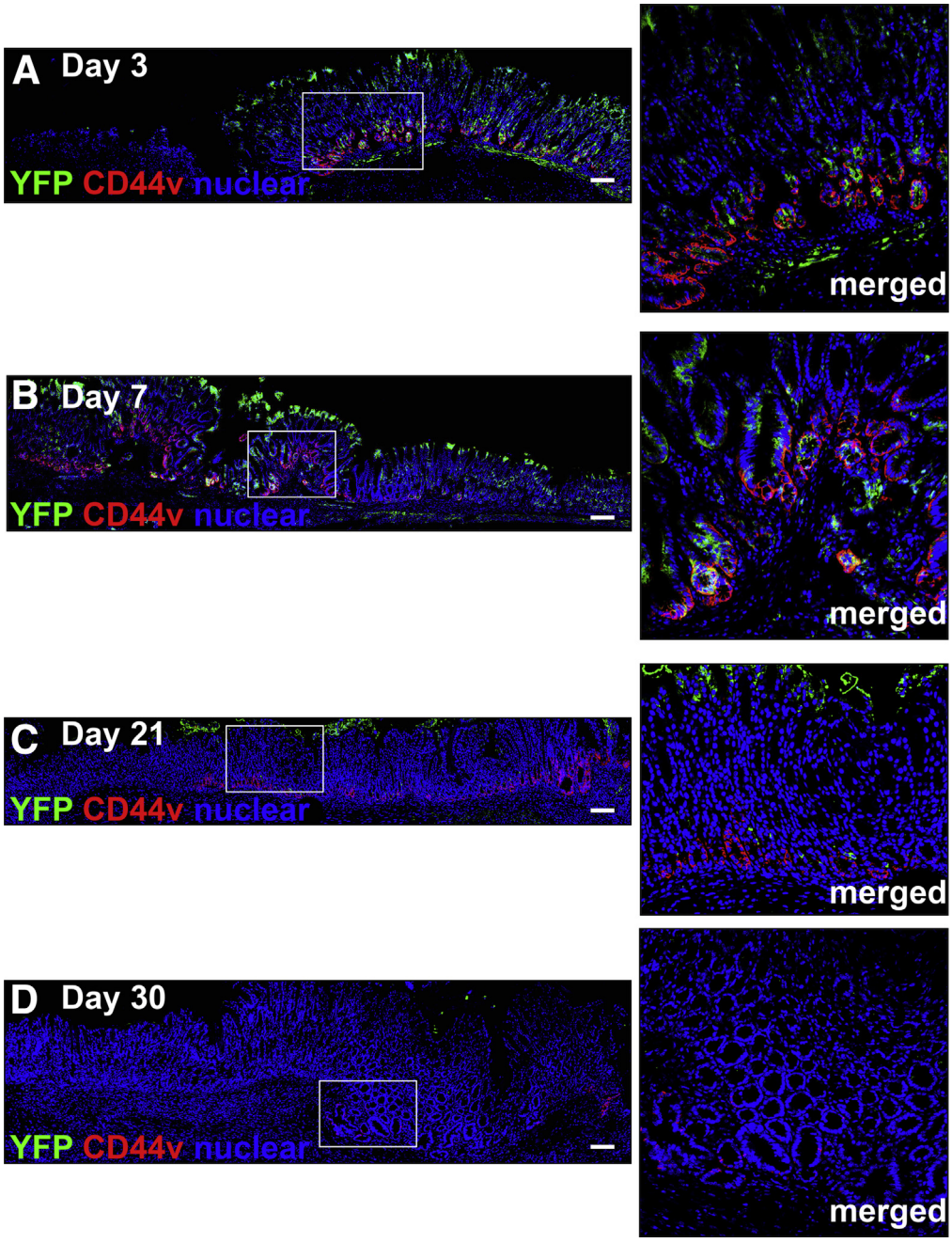

Figure 8. Engraftment of organoids within the mouse gastric epithelium. Immunostaining of YFP+ organoid-derived cells (green) and CD44v (red) within the ulcerated tissue of aged mice transplanted with gastric organoids at (*A*) 3, (*B*) 7, (*C*) 21, and (*D*) 30 days after injury. *Scale bars*: 50 μm.

Organoid transplantation also appeared to accelerate repair in the stomachs of younger mice, as shown by the significantly smaller ulcer sizes at 1 and 3 days after injury (Figure 10*D*). Although 30 days after injury the ulcer had healed by gross morphology, whole mount tissue immunostaining of the stomach showed an area where parietal cells had not regenerated (Figure 10*D*). Notably, this area of unregenerated epithelium was smaller in mouse stomachs transplanted with organoids 30 days after injury (Figure 10*D*). Immunofluorescence staining in young mice transplanted with organoids showed the re-expression of surface mucous pit, parietal, and endocrine cells within the repaired epithelium 30 days after injury (Figure 10*F*). Specifically, parietal cell numbers, although not comparable with uninjured tissue, were significantly greater than cell numbers counted in young untransplanted injured stomachs 30 days after injury (Figures 3*D* and 10*D*).

SPEM Lineages in the Transplanted Aged Stomach May Be Derived From Gastric Organoids

A heat map comparing the expression profiles of native fundic tissue and organoids showed higher levels of a number of transcripts within the organoids that were implicated in the emergence of SPEM (Figure 11*A* and *B*). Figure 11*A* and *B*

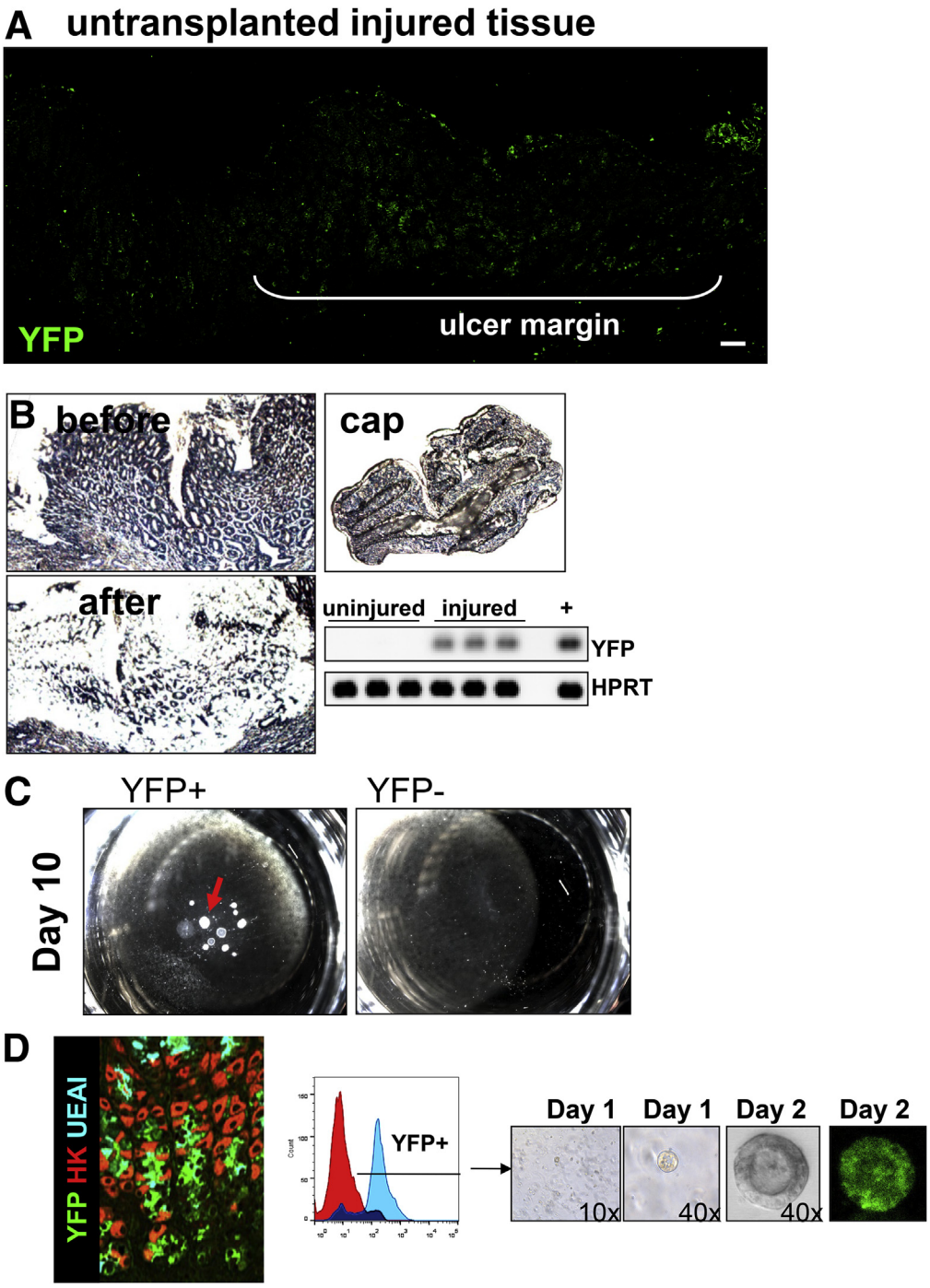

Figure 9. YFP expression in gastric epithelium of organoid transplanted mice. (*A*) Immunofluorescence staining using an antibody against YFP in untransplanted mice 7 days after injury. *Scale bars*: 50 μm. (*B*) YFP expression by RT-PCR using RNA prepared from laser capture microdissection of ulcerated and intact epithelium from stomachs 7 days after injury and gastric organoid transplantation. CAP, captured tissue. (*C*) Single cells flow sorted from stomach tissue of aged transplanted mice for YFP+ and YFP- grown in culture for 10 days. (*D*) Fluorescence-activated cell sorting (FACS) histogram depicting YFP+ single-cell population isolated from gastric tissue of aged mice transplanted with gastric organoids. YFP+ single cells were collected from the gastric glands 5 months after injury and gastric organoid transplantation and used to generate YFP+ gastric organoids in culture.

suggest that, compared with native tissue, the organoids showed a prominent up-regulation of a number of transcripts including Dmbt1, Clu,[29] Mad2l1, Cftr, Wfdc2 (HE4), and Gpx2, indicative of SPEM development.[9,23] qRT-PCR data validated the increase in Clu, Wfdc2 (HE4), and TFF2 observed in the organoids compared with isolated glands (Figure 11*C*–*E*). Although organoids derived from aged mouse stomachs showed an induction in Clu and HE4, these responses were significantly lower compared with the organoids derived from young mouse stomachs (Figure 11*C*–*E*). Collectively, these data support the conclusion that the SPEM lineages contributing to wound healing in the transplanted aged stomach may be derived from the gastric organoids.

Emergence of SPEM in Gastric Ulcers of Young Patients

Our data show that there is an emergence of SPEM cells at the base of the glands at the ulcer margin, which may play a fundamental role in the regeneration of the gastric

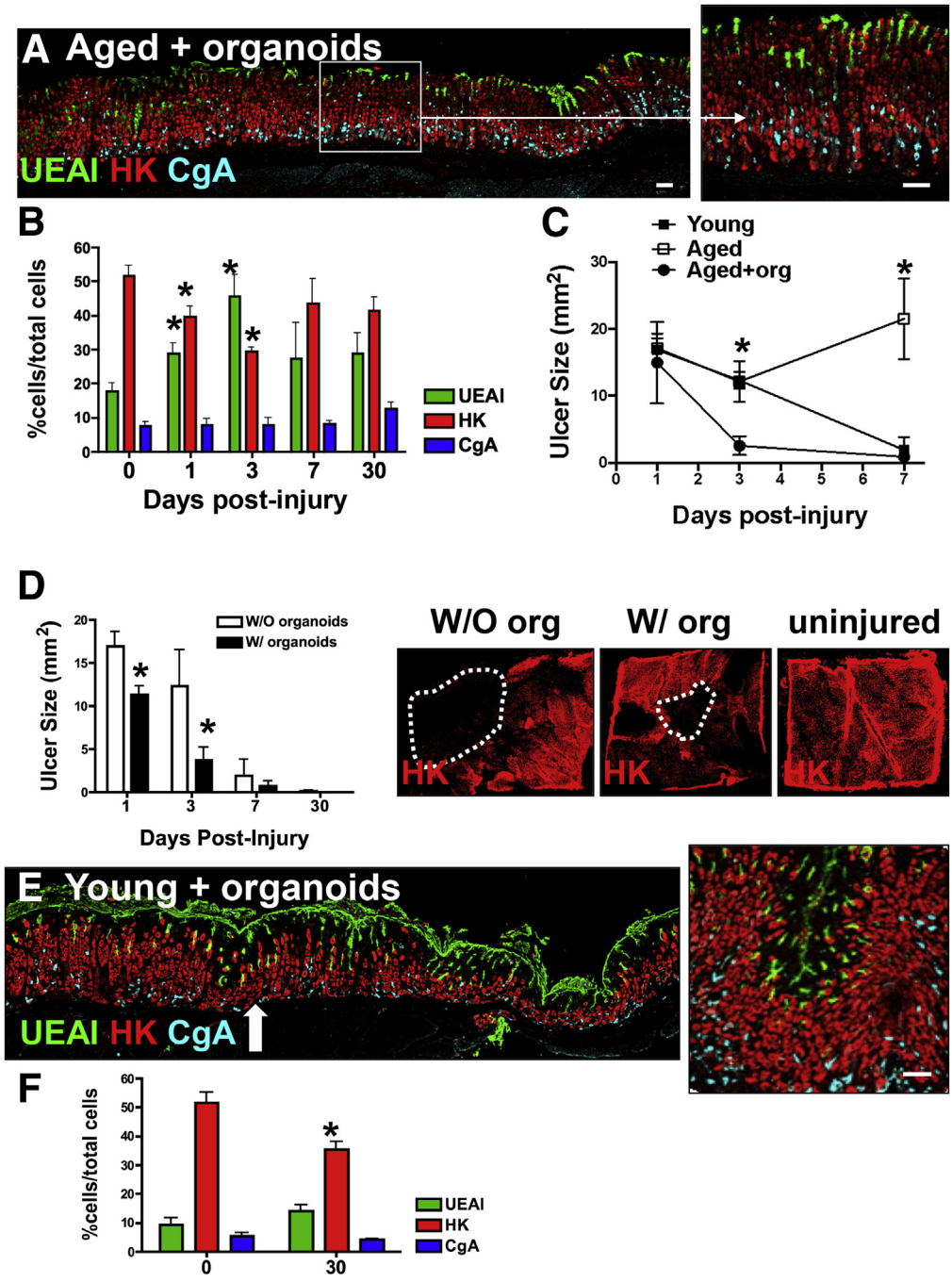

Figure 10. Organoid-derived SPEM cell lineages may contribute to wound healing in the aged stomach. (*A*) Immunofluorescence staining of ulcerated gastric tissue of aged mice transplanted with gastric organoids 30 days after injury. A lectin specific for surface mucous pit cells (UEAI, green) and antibodies specific for parietal cells (HK, red) and endocrine cells (CgA, blue) were used to identify cell lineages. *Scale bars*: 50 μm. (*B*) Quantification of UEAI+, HK+, and CgA+ cells within the damaged epithelium of aged mice transplanted with gastric organoids 1–30 days after injury. Data are presented as means ± SEM, N = 3–4 mice per time point. *$P < .05$ compared with day 0, determined by 1-way analysis of variance. (*C*) Ulcer measurements from young (black), aged (red), and aged mice transplanted with gastric organoids (green) at 1, 3, and 7 days after injury. Data are expressed as means ± SEM. *$P < .05$ compared with aged transplanted with organoids using 1-way analysis of variance, N = 3–10 mice per time point. (*D*) Ulcer measurements from young mice without (W/O) or with (W/) organoid transplantation at 1, 3, 7, and 30 days after injury. Data are expressed as means ± SEM. *$P < .05$ compared with young untransplanted mice using 1-way analysis of variance, N = 4 mice per time point. Whole mount immunofluorescence staining to identify parietal cells using antibody specific for H+K+–adenosine triphosphatase in stomach tissue collected from young mice without or with organoid transplantation or uninjured 30 days after injury. (*E*) Sections of injured gastric tissue collected from young mice were immunostained transplanted with organoids for UEAI (surface mucous pit cells, green), HK (parietal cells, red), and CgA (endocrine cells, blue) 30 days after injury. *Arrow* indicates area of injury. *Scale bar*: 50 μm. (*F*) Morphometric analysis of UEAI, HK, and CgA-positive cells per field in uninjured stomach tissue and ulcerated tissue 30 days after injury. Data are expressed as means ± SEM. *$P < .05$ compared with young untransplanted mice using 1-way analysis of variance, N = 4 mice per time point.

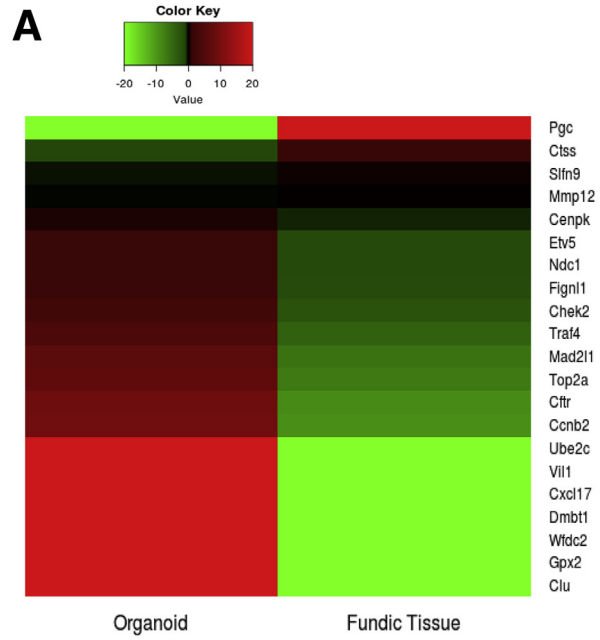

B

Gene Symbol	Fold Change
Pgc	0.001
Ctss	0.173
Slfn9	0.482
Wfdc21*	0.329
Mmp12	0.463
Cenpk	2.127
Etv5	2.506
Ndc1	2.342
Fignl1	4.923
Chek2	2.904
Traf4	1.510
Mad2l1	5.831
Top2a	3.544
Cftr	306.699
Ccnb2	8.514
Ube2c	5.154
Vil1	10.078
Cxcl17	2.965
Dmbt1	16.300
Gpx2	29.988
Clu	13.969

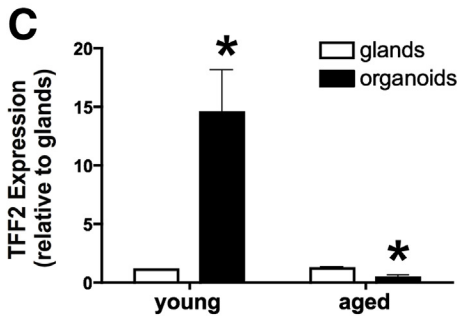

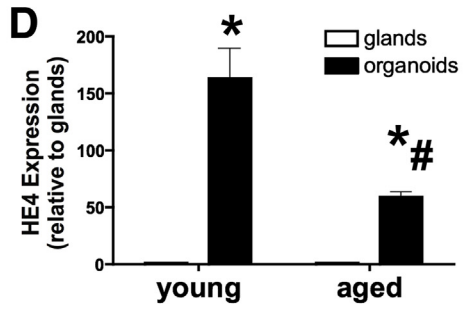

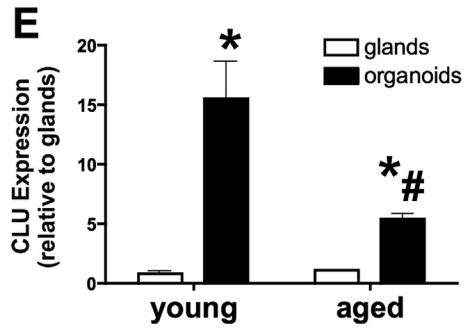

Figure 11. Expression of SPEM markers in gastric organoid cultures. (*A*) Heat map of centered reads per kilobase per million values depicting gene expression changes in SPEM-associated genes using RNA isolated from organoid and native fundic tissue. (*B*) Table showing fold change of transcripts associated with the emergence or progression of SPEM. qRT-PCR was performed using RNA isolated from glands and organoids derived from young and aged mouse stomachs. Shown is the average fold change of SPEM-associated genes (*C*) TFF2, (*D*) clusterin (CLU), and (*E*) HE4. Shown is the average fold change of SPEM-associated genes TFF2, clusterin (CLU), and HE4. *$P < .05$ compared with glands or normal glands expression. #$P < .05$ compared with young organoids using either the Student *t* test or 1-way analysis of variance.

epithelium. To examine the emergence of SPEM during gastric ulceration in the human stomach, the expression of the SPEM marker CD44v[27] was investigated in a gastric ulcer tissue array of patients at varying ages (Figure 12). CD44v-positive glands co-expressing TFF2 and GSII were observed within the ulcerated area of 100% of 6 young patients between 27 and 38 years of age (Figure 12*A* and *B*). However, in patients older than 55 years of age (total, 18 patients), CD44v expression was not detected in any of the 18 sections despite GSII/TFF2 co-expressing glands within the ulcerated area (Figure 12*C* and *D*). These data suggest that in young patients (age, <38 y) there is a robust expression of SPEM within the gastric ulcer, while within the aging stomach CD44v expressing SPEM was absent.

Engraftment of Human-Derived Gastric Organoids in NOD SCID γ Mouse Stomachs

According to the data presented in our study, gastric organoids offer an attractive source of cells for transplants to potentially treat gastrointestinal disease. Therefore, to identify whether human-derived gastric organoids are transplantable, we first developed gastric organoids from human fundic stomach tissue (Figure 13*A*). Human-derived fundic

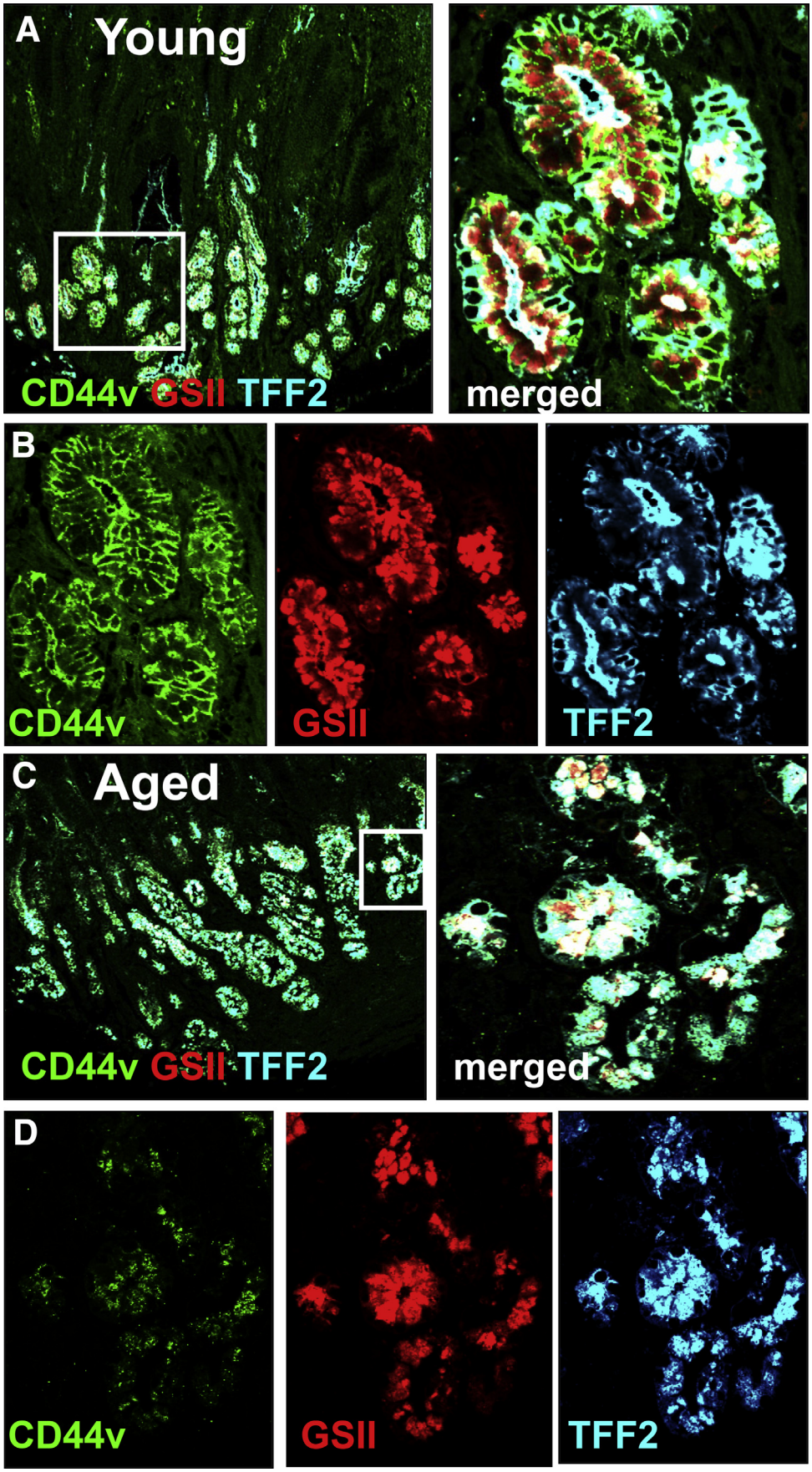

Figure 12. Emergence of SPEM in gastric ulcers of young patients. Immunofluorescence staining using human-specific antibodies for CD44v (hCD44v, green), TFF2 (hTFF2, blue), and GSII (red) in gastric ulcer tissue collected from (*A* and *B*) young (age, 27 y) and (*C* and *D*) aged (age, 65 y) patients. (*B* and *D*) Higher magnification of SPEM in the ulcer margin is shown.

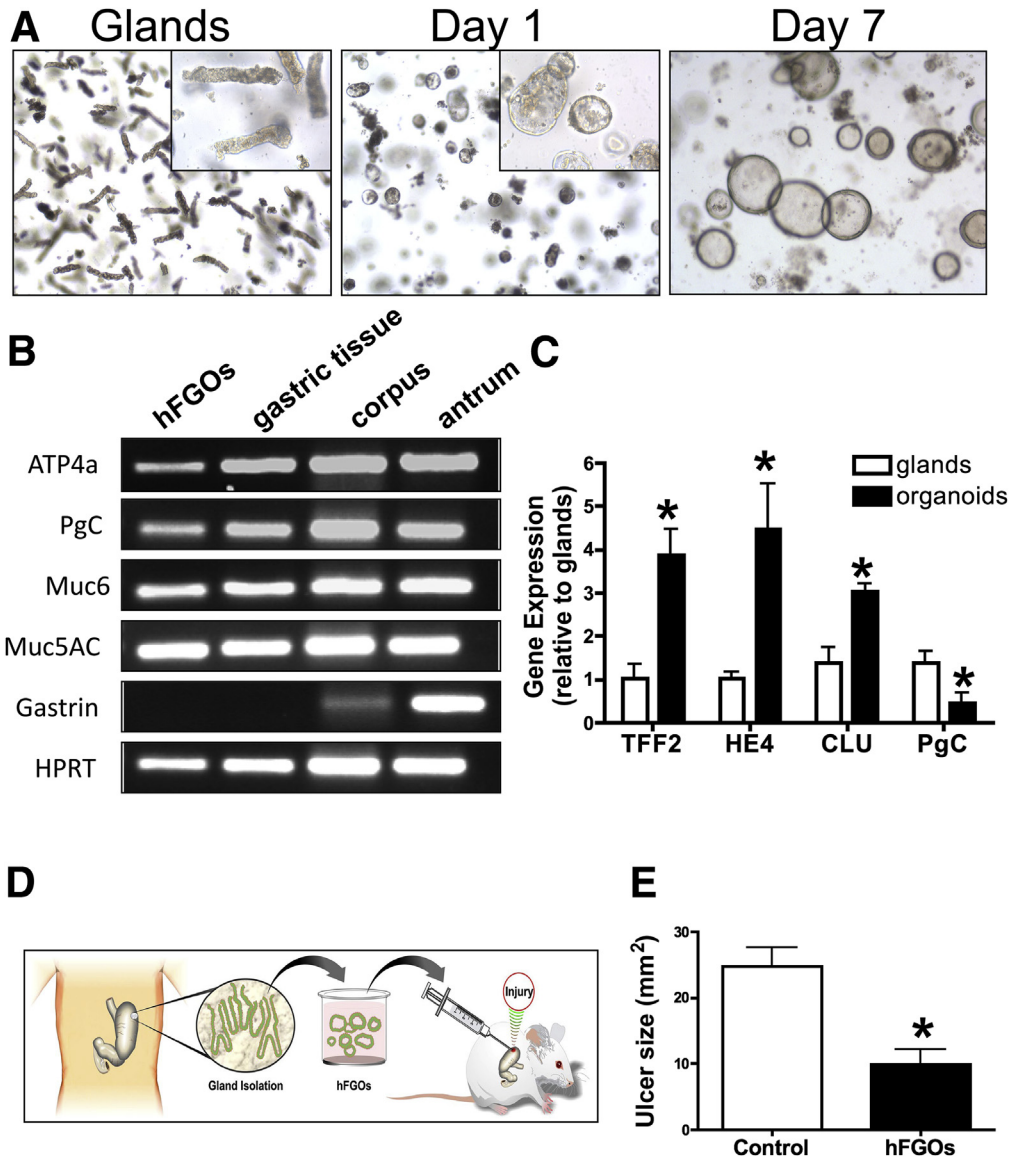

Figure 13. Human-derived gastric organoids. (*A*) Gastric glands isolated from the fundus of human stomach grew in vitro to form gastric organoids. (*B*) Expression of genes for the gastric cell lineage markers: parietal cells (ATP4a), chief cells (pepsinogen [PgC]), surface mucous pit cells (Muc5AC), and mucous neck cells (Muc6) in the hFGOs, gastric tissue, human corpus, and antrum. Gastrin (Gast) was not detected in the hFGOs, indicating that the hFGOs are derived from the fundus. (*C*) hFGOs also expressed SPEM markers Clu, HE4, TFF2, and PgC. N = 4 samples or cultures per group, data are expressed as fold change relative to glands. **P* < .05 compared with glands determined by 1-way analysis of variance. (*D*) Experimental protocol. (*E*) Ulcer sizes for untransplanted NOD SCID γ mice (control) and hFGO transplanted mice 7 days after injury. **P* < .05 compared with control determined by the Student *t* test, N = 4–8 mice per group.

gastric organoids (hFGOs) were generated from gastric glands dissociated from fundic tissue of the stomach (Figure 13*A*). Fundic glands formed cyst-like structures visible within 1 day of culture that grew over the subsequent 7 days, at which time the hFGOs were used for transplants (Figure 13*A*). We determined the gene expression of gastric-specific cell lineage markers before the first passage. The hFGOs expressed messenger RNA for mucin 5AC (surface mucous pit cells), mucin 6 (mucous neck cells/SPEM), pepsinogen C (zymogen/chief cells), and ATP4a (parietal cells), as detected by PCR that was comparable with the expression profile of human corpus tissue (Figure 13*B*). The expression of gastrin (G cells), which is specific to antrum, was not detected in the hFGOs (Figure 13*B*). Consistent with the emergence of SPEM and the expression profile of the mouse-derived gastric organoids, markers Clu, HE4, and TFF2 also were expressed and up-regulated in the hFGOs when compared with isolated glands (Figure 13*C*).

The hFGOs were harvested after 7 days in culture and transplanted into NOD SCID γ mice after ulcer induction (Figure 13*D*). At 7 days after injury, NOD SCID γ mice transplanted with the hFGOs had a significantly reduced ulcer size when compared with the untransplanted control group (Figure 13*E*). Expression of human-specific histone was localized within the regenerating gastric glands and co-expressed SPEM marker human-specific CD44v (Figure 14*A*–*E*). Engraftment of organoids within the submucosa was observed 60 days after injury, as shown by the expression of human-specific, histone-positive nuclei (Figure 14*F*). Collectively, these data show that human-derived gastric organoids are indeed transplantable and may offer a source of cells to promote gastric tissue repair in response to injury.

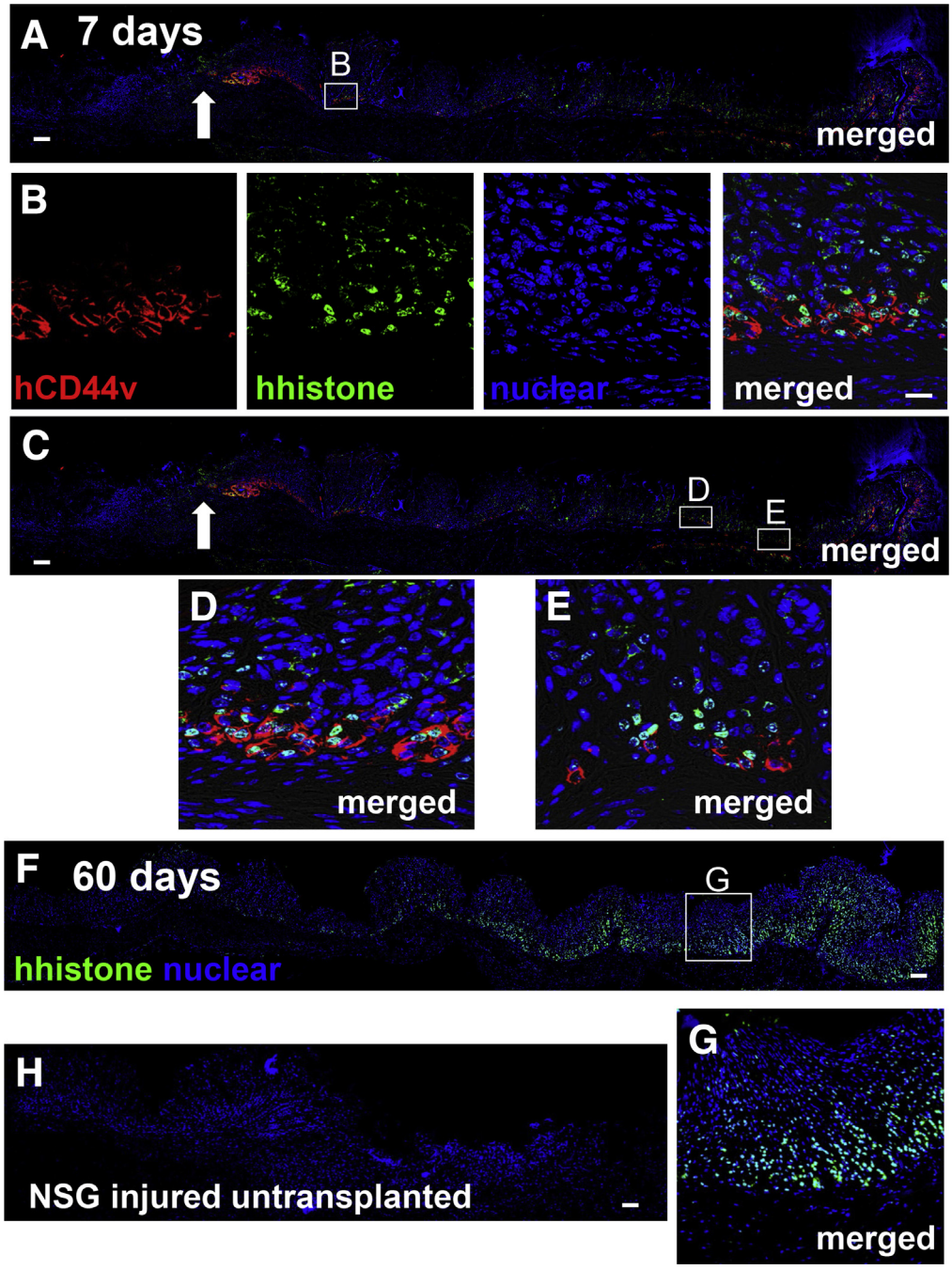

Figure 14. Engraftment of hFGOs in NOD SCID γ mouse stomach after ulceration. (*A–E*) Immunofluorescence staining using human-specific antibodies for CD44v (hCD44v, green) and histone (histone) in gastric tissue from NOD SCID γ mice transplanted with hFGOs 7 days after injury. (*B*, *D*, and *E*) Higher magnification of regenerating epithelium in the ulcer margin is shown in *insets*. (*F*) Immunofluorescence staining for human-specific histone in gastric tissue from NOD SCID γ mice transplanted with hFGOs 60 days after injury. (*G*) Higher magnification is shown. (*H*) Immunofluorescence staining for human-specific histone in gastric tissue from untransplanted NOD SCID γ mice. *Arrows* indicate area of injury. *Scale bars*: 50 μm.

Discussion

Our data show the development of SPEM during gastric repair in response to injury. During repair we observed an up-regulation of transcripts indicative of emerging SPEM cells.[23] The RNA sequencing data were validated by qRT-PCR, and immunofluorescence staining showed the co-expression of IF, TFF2, and GSII lectin within the regenerating gastric epithelium.[11,24,25] CD44v also was expressed within SPEM glands of the ulcerated tissue in both mouse and human beings. In support of our observation, it has been reported that CD44v is expressed de novo in SPEM and results in the up-regulation of glutamate-cystine transporter glutamate-cystine transporter activity.[27] Our immunofluorescence staining showing decreased expression of CD44v in the human aged stomach would suggest a plausible role of CD44v during regeneration of the gastric epithelium that is compromised with aging. CD44 expression also is increased in the human bronchial epithelium, where it may play a functional role in repair via regulation of cell motility and proliferation.[30] However, we report the potential role of CD44v in gastric repair.

SPEM typically has been shown to arise as a result of parietal cell loss, leading to the transdifferentiation of mature chief cells into metaplastic mucus-secreting cells.[8] *Helicobacter* infection and parietal cell–specific protonophores (DMP-777 and L635) are known inducers of SPEM.[8,9] Although an earlier study reported the emergence of TFF2 expression at the ulcer margin,[31] we report the induction of SPEM after gastric ulceration. SPEM was identified in the ulcer margin in the regenerating gastric glands and disappeared when the mucosa returned to its normal compendium of cell lineages, suggesting a possible role for SPEM in ulcer repair. Emerging SPEM cells were localized to the base of the ulcer margin, similar to where the ulcer associated cell lineages have been described previously during repair in the intestine.[32] Our data suggest that SPEM may represent the major reparative lineage responsible for wound healing after severe gastric ulceration.

Although ulcers induced in aged mice led to aberrant repair, as evidenced by the formation of foveolar hyperplasia within the injured tissue, organoid transplantation restored normal glandular architecture in these mice. These data are consistent with findings showing impaired angiogenesis, decreased prostaglandin biosynthesis, and delayed injury healing in the gastric mucosa of aging rats.[2,33,34] Here, we show that engraftment of cells through the transplantation of gastric organoids contributes to ulcer repair in aged mice. Previous studies have shown organoid engraftment and repair in the mouse intestine. Yui et al[35] have shown that organoids derived from a single Lgr5+ colon stem cell are transplantable, engrafting within a superficially damaged mouse colon. This organoid engraftment was shown to be beneficial to the recipient mice.[35] In addition, Fordham et al[36] showed that after transplantation into a colonic injury model, in vitro expanded fetal intestinal progenitors contribute to epithelial regeneration. Our study reports that mouse- and human-derived organoids are transplantable in gastric tissue and are beneficial for repair of ulcer damage. We are still in the preliminary stages of investigating the engraftment and differentiation of organoids transplanted into the gastric epithelium. However, taken together, these results indicate that transplantation of organoids may provide SPEM lineage cells that can promote repair in the aged stomach.

References

1. Salles N. Is stomach spontaneously ageing? Pathophysiology of the ageing stomach. Best Pract Res Clin Gastroenterol 2009;23:805–819.
2. Ahluwalia A, Jones MK, Deng X, et al. An imbalance between VEGF and endostatin underlies impaired angiogenesis in gastric mucosa of aging rats. Am J Physiol Gastrointest Liver Physiol 2013;305:G325–G332.
3. Ahluwalia A, Jones MK, Szabo S, et al. Aging impairs transcriptional regulation of vascular endothelial growth factor in human microvascular endothelial cells: implications for angiogenesis and cell survival. J Physiol Pharmacol 2014;65:209–215.
4. Tarnawski AS, Ahluwalia A, Jones MK. Angiogenesis in gastric mucosa: an important component of gastric erosion and ulcer healing and its impairment in aging. J Gastroenterol Hepatol 2014;29:112–123.
5. Jones JI, Hawkey CJ. Physiology and organ-related pathology of the elderly: stomach ulcers. Best Pract Res Clin Gastroenterol 2001;15:943–961.
6. Farinati F, Cardin F, Di Mario F, et al. Gastric ulcer and stomach aging: pathophysiology and clinical implications. Gerontology 1988;34:297–303.
7. Hinsull SM. Effect of colloidal bismuth subcitrate on age related gastric lesions in the rat. Gut 1991;32:355–360.
8. Nam KT, Lee HJ, Sousa JF, et al. Mature chief cells are cryptic progenitors for metaplasia in the stomach. Gastroenterology 2010;139:2028–2037.
9. Weis VG, Sousa JF, LaFleur BJ, et al. Heterogeneity in mouse spasmolytic polypeptide-expressing metaplasia lineages identifies markers of metaplastic progression. Gut 2013;62:1270–1279.
10. Petersen CP, Weis VG, Nam KT, et al. Macrophages promote progression of spasmolytic polypeptide-expressing metaplasia after acute loss of parietal cells. Gastroenterology 2014;146:1727–1738.
11. Nomura S, Yamaguchi H, Ogawa M, et al. Alterations in gastric mucosal lineages induced by acute oxyntic atrophy in wild-type and gastrin-deficient mice. Am J Physiol Gastrointest Liver Physiol 2005; 288:G362–G375.
12. Mahé MM, Aihara E, Schumacher MA, et al. Establishment of gastrointestinal epithelial organoids. Curr Protoc Mouse Biol 2013;3:217–240.
13. Schumacher MA, Aihara E, Feng R, et al. The use of murine-derived fundic organoids in studies of gastric physiology. J Physiol 2015;593:1809–1827.
14. Feng R, Aihara E, Kenny S, et al. Indian hedgehog mediates gastrin-induced proliferation in stomach of adult mice. Gastroenterology 2014;147:655–666.
15. Bertaux-Skeirik N, Feng R, Schumacher MA, et al. CD44 plays a functional role in Helicobacter pylori-induced epithelial cell proliferation. PLoS Pathog 2015; 11:e1004663.
16. Okabe S, Amagase K. An overview of acetic acid ulcer models–the history and state of the art of peptic ulcer research. Biol Pharm Bull 2005;28:1321–1341.
17. Trapnell C, Pachter L, Salzberg SL. TopHat: discovering splice junctions with RNA-Seq. Bioinformatics 2009; 25:1105–1111.
18. Huber W, Carey VJ, Gentleman R, et al. Orchestrating high-throughput genomic analysis with Bioconductor. Nat Methods 2015;12:115–121.
19. Anders S, McCarthy DJ, Chen Y, et al. Count-based differential expression analysis of RNA sequencing data using R and Bioconductor. Nat Protoc 2013;8: 1765–1786.
20. Anders S, Huber W. Differential expression analysis for sequence count data. Genome Biol 2010;11:R106.
21. Subramanian A, Tamayo P, Mootha VK, et al. Gene set enrichment analysis: a knowledge-based approach for interpreting genome-wide expression profiles. Proc Natl Acad Sci U S A 2005;102:15545–15550.
22. Weis VG, Petersen CP, Mills JC, et al. Establishment of novel in vitro mouse chief cell and SPEM cultures

identifies MAL2 as a marker of metaplasia in the stomach. Am J Physiol Gastrointest Liver Physiol 2014;307:G777–G792.
23. Nozaki K, Ogawa M, Williams JA, et al. A molecular signature of gastric metaplasia arising in response to acute parietal cell loss. Gastroenterology 2008;134:511–522.
24. Nam KT, Lee HJ, Mok H, et al. Amphiregulin-deficient mice develop spasmolytic polypeptide expressing metaplasia and intestinal metaplasia. Gastroenterology 2009;136:1288–1296.
25. Yoshizawa N, Takenaka Y, Yamaguchi H, et al. Emergence of spasmolytic polypeptide-expressing metaplasia in Mongolian gerbils infected with Helicobacter pylori. Lab Invest 2007;87:1265–1276.
26. Ramsey VG DJ, Chen CC, Stappenbeck TS, et al. The maturation of mucus-secreting gastric epithelial progenitors into digestive-enzyme secreting zymogenic cells requires Mist1. Development 2007;134:211–222.
27. Wada T, Ishimoto T, Seishima R, et al. Functional role of CD44v-xCT system in the development of spasmolytic polypeptide-expressing metaplasia. Cancer Sci 2013;104:1323–1329.
28. Miyawaki A, Nagai T, Mizuno H. Imaging intracellular free Ca2+ concentration using yellow cameleons. Cold Spring Harb Protoc 2013;2013:11.
29. Howlett M, Giraud AS, Lescesen H, et al. The interleukin-6 family cytokine interleukin-11 regulates homeostatic epithelial cell turnover and promotes gastric tumor development. Gastroenterology 2009;136:967–977.
30. Leir SH, Baker JE, Holgate ST, et al. Increased CD44 expression in human bronchial epithelial repair after damage or plating at low cell densities. Am J Physiol Lung Cell Mol Physiol 2000;278:L1129–L1137.
31. Kikuchi M, Nagata H, Watanabe N, et al. Altered expression of a putative progenitor cell marker DCAMKL1 in the rat gastric mucosa in regeneration, metaplasia and dysplasia. BMC Gastroenterol 2010;10:65.
32. Wright NA. Aspects of the biology of regeneration and repair in the human gastrointestinal tract. Philos Trans R Soc Lond B Biol Sci 1998;353:925–933.
33. Uchida M, Kawano O, Misaki N, et al. Healing of acetic acid-induced gastric ulcer and gastric mucosal PGI2 level in rats. Dig Dis Sci 1990;35:80–85.
34. Lee M, Feldman M. Age-related reductions in gastric mucosal prostaglandin levels increase susceptibility to aspirin-induced injury in rats. Gastroenterology 1994;107:1746–1750.
35. Yui S, Nakamura T, Sato T, et al. Functional engraftment of colon epithelium expanded in vitro from a single adult Lgr5+ stem cell. Nat Med 2012;18:618–623.
36. Fordham RP, Yui S, Hannan NR, et al. Transplantation of expanded fetal intestinal progenitors contributes to colon regeneration after injury. Cell Stem Cell 2013;13:734–744.

Received January 28, 2016. Accepted May 6, 2016.

Correspondence
Address correspondence to: Yana Zavros, PhD, Department of Molecular and Cellular Physiology, University of Cincinnati College of Medicine, 231 Albert B. Sabin Way, Room 4255 MSB, Cincinnati, Ohio 45267-0576. e-mail: yana.zavros@uc.edu; fax: (513) 558-5738; or James R. Goldenring, MD, PhD, Vanderbilt University Medical Center, Medical Research Building IV, Room 10435-G, 2213 Garland Avenue, Nashville, Tennessee 37232. e-mail: jim.goldenring@vanderbilt.edu; fax: (615) 343-1591.

Acknowledgments
The authors thank Jenny Chen (Department of Environmental Health, Division of Biostatistics and Bioinformatics, University of Cincinnati College of Medicine) for her assistance with submitting the data to a public repository (GEO website). The authors also thank Chet Closson (Laboratory Manager, Live Microscopy Core, Department of Molecular and Cellular Physiology, University of Cincinnati) for his assistance with imaging slides and Andrea Matthis for technical assistance with the whole mount tissue immunostaining.

Conflicts of interest
The authors disclose no conflicts.

Funding
This work was supported by National Institutes of Health grants 1R01DK083402 (Y.Z.) and RO1 DK101332 (J.R.G.), the College of Medicine Bridge Funding Program (Y.Z.), the University of Cincinnati Graduate School Dean's Fellowship (A.C.E.), and a Department of Veterans Affairs Merit Review Award (2I01BX000930) (J.R.G.). This project also was supported in part by PHS grant P30 DK078392 (Integrative Morphology Core) and National Institutes of Health grant AR-47363 (Research Flow Cytometry Core in the Division of Rheumatology of the Digestive Diseases Research Core Center in Cincinnati).